AECL-7797

ATOMIC ENERGY OF CANADA LIMITED

L'ENERGIE ATOMIQUE DU CANADA, LIMITEE

DYNAMIC RESPONSE OF UNDERGROUND OPENINGS IN DISCONTINUOUS ROCK

REPONSE DYNAMIQUE DES ESPACES SOUTERRAINS DANS UNE ROCHE DISCONTINUE

H. W. Asmis *

* Ontario Hydro

Whiteshell Nuclear Research Establishment

Etablissement de recherches nucléaires de Whiteshell

Pinawa, Manitoba R0E 1L0

February 1984 février

10

ATOMIC ENERGY OF CANADA LIMITED

DYNAMIC RESPONSE OF UNDERGROUND OPENINGS IN DISCONTINUOUS ROCK

by

H.W. Asmis*

* Geotechnical Engineering Department, Ontario Hydro.

Whiteshell Nuclear Research Establishment
Pinawa, Manitoba ROE 1LO
1984 February

AECL-7797

RÉPONSE DYNAMIQUE DES ESPACES SOUTERRAINS DANS UNE ROCHE DISCONTINUE

par

H.W. Asmis*

RÉSUMÉ

Le présent rapport examine le comportement des espaces souterrains dans une roche discontinue en réponse à des ondes sismiques associées aux tremblements de terre ou à l'éclatement de la roche. Une recherche documentaire a révélé que les structures souterraines bien construites, telles qu'enceintes d'évacuation de déchets de combustible nucléaire, centrales nucléaires et réservoirs d'eau pompée souterrains, sont extrêmement résistantes aux dommages causés par les mouvements sismiques. Pour compléter ces résultats qualitatifs, il a été nécessaire d'examiner les mécanismes de base de la progression des mouvements sismiques dans son ensemble, à partir de la production des ondes et de leur propagation, jusqu'à leur interaction avec l'espace souterrain. Grâce à cette étude, on a pu établir que les contraintes exercées seraient faibles par rapport aux contraintes d'excavation, à moins qu'un événement sismique ne se produise à proximité des installations, étant donné que les ondes de contraintes élevées s'atténuent rapidement en traversant la roche. De même un tremblement de terre peut, lui aussi, produire des accélérations extrêmement élevées mais la quantité maximale de contraintes qu'il peut engendrer sera limitée. Cependant, la véritable nature précise des mouvements sismiques souterrains est une question qui n'est pas encore résolue, bien que l'on s'attende à ce qu'il y ait une réduction des mouvements de pointe en fonction de la profondeur, par suite de l'effet de la surface libre de la terre.

Étant donné que l'espace souterraine se trouve en régime de contrainte, une rupture dynamique le long d'un point de contrainte ou de toute autre discontinuité existants peut s'avérer être un mécanisme de défaillance sérieux. Un tel événement pourrait être déclenché par des mouvements sismiques ou se produire spontanément. Des simulations de différences finies sur ordinateur reproduisant des ondes sismiques frappant une caverne ont indiqué que les contraintes sismiques pourraient difficilement provoquer des mécanismes de défaillance par glissement. Le modèle permettait la rupture spontanée de discontinuités, ce qui a fait constater que les paramètres d'adhésion, de déplacement critique et d'angle de friction minimal ont une influence marquée sur la stabilité.

* Le Département d'ingénierie géotechnique de l'Ontario Hydro

L'Énergie Atomique du Canada, Limitée
Établissement de recherches nucléaires de Whiteshell
Pinawa, Manitoba ROE 1LO
1984 février

AECL-7797

DYNAMIC RESPONSE OF UNDERGROUND OPENINGS IN DISCONTINUOUS ROCK

by

H.W. Asmis*

ABSTRACT

This report examines the behaviour of underground openings in discontinuous rock in response to seismic waves associated with either earthquakes or rock bursts. A literature search revealed that well-constructed underground structures, such as would be expected for nuclear fuel waste disposal vaults, underground pumped-storage or nuclear plants, have an extremely high resistance to damage from seismic motion. To complement these qualitative results, it was necessary to examine the basic mechanisms of the entire progression of seismic motion, from wave generation and propagation, to wave interaction with the underground opening. From these investigations, it was found that unless a seismic event occurs very close to the installation, the stresses generated will be low with respect to the excavation stresses, because high stress waves are rapidly attenuated in travelling through rock. As well, an earthquake may generate extremely high accelerations, but is limited in the maximum amount of stress that it can create. The question, however, of the actual specific nature of underground seismic motions still remains essentially unanswered, although it is expected that there is a reduction in peak motions with depth due to the effect of the free surface of the earth.

Since the underground opening is in a stressed regime, dynamic rupturing along an existing stressed joint or other discontinuity may prove to be a failure mechanism of concern. Such an event could be triggered by seismic motions or could occur spontaneously. Finite-difference computer simulations of seismic waves striking a cavern indicated that it would be difficult for seismic stresses to trigger slip-failure mechanisms. Discontinuities were allowed to rupture spontaneously in the model and it was found that the adhesion parameters of critical displacement and minimum angle of friction have a significant influence on stability.

* Geotechnical Engineering Department, Ontario Hydro.

Atomic Energy of Canada Limited
Whiteshell Nuclear Research Establishment
Pinawa, Manitoba ROE 1LO
1984 February

AECL-7797

CONTENTS

1. INTRODUCTION

This study constitutes part of the Ontario Hydro contribution to the Canadian Nuclear Fuel Waste Management Program, carried out under the auspices of Atomic Energy of Canada Limited, Whiteshell Nuclear Research Establishment. Examined in this report are aspects of the dynamic response of underground openings in discontinuous rock. The purpose of the study is to develop a methodology of analysis that may be applicable to a large range of engineering projects, such as underground nuclear fuel waste disposal vaults, underground nuclear plants, pumped storage schemes, and general rock excavations.

The reference area for the study is Ontario. Its rocks are characterized by prevalent high horizontal stresses and frequent jointing and faulting. As such, there are many unique problems related to seismicity and the dynamic stability of caverns. In particular, due to the high stresses, dynamic behaviour can be divided into two types: effects related to distant seismic sources, such as earthquakes; and effects related to near-cavern disruptive events, usually manifested as rock bursts.

2. BACKGROUND

Earthquakes damage engineered installations in a variety of ways. The most destructive effects are observed right at the source, especially if the displaced fault breaks the surface. Any structure straddling the fault, including tunnels crossing the fault, would be sheared apart by the high stresses that are necessary to shift so much earth and rock. Such surface fault displacements in rock, however, are primarily confined to active plate margins. In Ontario, therefore, seismic damage from tectonic earthquakes would be restricted to the effects of the seismic waves generated by these events.

The mechanisms for seismic damage to underground openings are significantly different than those for a surface structure, but since most experience on the effect of earthquakes has been gained on the surface of the earth, it is instructive to examine surface responses. When a surface structure is being shaken by seismic waves, it begins to vibrate primarily at one or more natural frequencies that are unique for that building. In fact, any type of excitation, such as wind gusts or impact, would cause that building to quiver or shake at those natural frequencies. In much the same manner, a soil deposit overlying rock will shake at certain defined frequencies in response to many forms of excitation, such as explosions or earthquakes. The phenomenon is known as resonance, and is a common property of all geometric forms of matter, including the entire earth, which resonates or "rings" at very low frequencies after great earthquakes.

Most seismic damage occurs when the natural resonant frequencies of the soil and the building approximate one another. Several case histories of cities affected by earthquakes show that the chief damage was confined to areas where the resonant frequencies of the soil matched those of the more severely damaged buildings. Other damage is usually caused by

actual shifting of the soil itself, either under foundations or in landslides. If all cases of damage involving soil-structure interaction were removed from consideration, there would be few incidences of seismic damage left. A case in point is the great Alaska earthquake of 1964 (magnitude, M = 7.2). The city of Anchorage, located on soil, was severely damaged. In the nearby town of Whittier, which was closer to the source, it was noted (Kachadoorian, 1965) that loss of life was due solely to waves. Property damage was caused by phenomena such as a 1.6-m subsidence of the land mass, seismic shock, compaction and fracturing of unconsolidated deposits and fill, and fire. All facilities built on the slate and graywacke bedrock were damaged slightly or not at all, whereas most buildings on unconsolidated sediments or fill were damaged significantly by the seismic activity.

In Ontario, the Cornwall earthquake of 1944 (M = 5.6) produced essentially the same results. Drawing on an inventory of damage to buildings and cemeteries, it was observed (Berkey, 1945) that:

> "Virtually all badly disturbed or violently shaken or much damaged buildings or other structures are located on either loose silty outwash or silt-clay marine deposits. No buildings or other structures located on heavy glacial till were destroyed or badly damaged."

A recent re-examination of the Cornwall earthquake by the author and others (Asmis, 1981) has indicated that damage may have been primarily due to poor construction techniques, such as unmortared chimneys and, in the case of the local high school, an almost completely unbraced roof structure. Damage also appeared to be correlated with soil deposits.

Strategies to minimize seismic damage have been to avoid soil-structure interaction by making the structures stiffer and by employing better construction techniques. Unfortunately, it is not always possible to choose better foundation materials, but it would appear that a highly damage-resistant structure would be stiff, strong and located on bedrock. This would be primarily to minimize resonance, and such structures, where they approach this ideal, have been known to survive very strong shaking. Of course, there is a way to carry this concept even further, and that is to build a stiff and strong structure underground in firm rock.

Although there is not a large amount of experience with regard to the seismic behaviour of underground openings, it is an essential first step to examine the history of the performance of tunnels during earthquakes. Dowding and Rozan (1978) have recently compiled a case history of rock tunnel response to earthquake shaking. The tunnel responses were compared with calculated peak ground motions for 71 cases to determine damage modes and the susceptibility of rock tunnels to such damage. Damage to tunnels was found to be generally manifested in one or more of the following forms:

(a) damage from earthquake-induced ground failure, such as liquefaction or landslides at tunnel portals;

(b) damage from fault displacement; and

(c) damage from ground "shaking", or ground vibration.

Damage due to ground failure and fault displacement can usually be avoided by prudent siting. This leaves only seismic motions as a concern.

Dowding and Rozan correlate tunnel damage with both surface peak acceleration and velocity, and mention that currently there is much debate over which is the more significant parameter with which to correlate damage. They then take the magnitude of the earthquake and its distance from the tunnel and use established attenuation relationships to derive the estimated surface velocities and accelerations. The peak values of acceleration or velocity are then plotted using a symbol indicating the type of damage encountered.

The three levels of response are divided according to the calculated peak surface motions, denoted by the terms "No Damage Zone," the "Minor Damage Zone" and the "Damage Zone" (see Figures 2.1 and 2.2). There are no reports of falling stones in unlined tunnels or cracking in lined tunnels, for peak accelerations up to 0.19 g. Up to 0.25 g, there are only a few incidences of minor cracking in concrete-lined tunnels. Between 0.25 g and 0.52 g, there was only one partial collapse, but it was associated with landsliding, and the tunnel was lined with masonry.

The observed damage is compared to Modified Mercalli (MM) intensity levels for above-ground structures. The "No Damage Zone", with acceleration up to 0.19 g, is equivalent to MM VI-VIII; the "Minor Damage Zone", with acceleration up to 0.5 g, is equivalent to MM VIII-IX. Therefore, at peak surface accelerations that normally result in heavy damage to above-ground structures (MM VIII-IX), there is only minor damage to tunnels.

In addition to the report by Dowding and Rozan, some earlier work on the effect of depth on seismic motion was performed by Duke and Leeds (1959), who state:

> "Qualitatively, these researches demonstrate experimentally the following effects at depth:
>
> (1) At short periods, surface displacements are larger than underground displacements.
>
> (2) The ratio of surface to underground displacement depends on the type of ground. It is greater for alluvium than for weathered rock. It may reach a value of at least 10.
>
> (3) For wave periods over one second, the ratio becomes comparatively small, approaching unity as the period increases.
>
> (4) There is a particular average period of incoming waves for which a given type of ground will provide a maximum ratio of surface to underground displacement. If the average period of incoming waves is not approximately equal to this particular period, the ratio will be materially smaller."

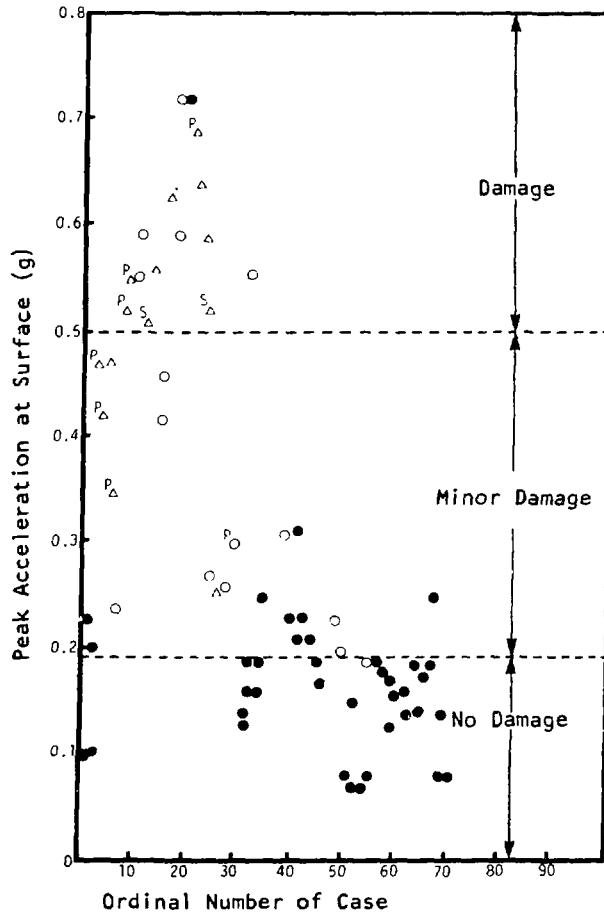

LEGEND

- ● No damage
- ○ Minor damage, due to shaking
- △ Damage from shaking
- $P_{\triangle}$ Near portal
- $S_{\triangle}$ Shallow cover

Fig. 2.1 CALCULATED PEAK SURFACE ACCELERATIONS AND ASSOCIATED DAMAGE OBSERVATIONS
(from Dowding and Rozan, 1978)

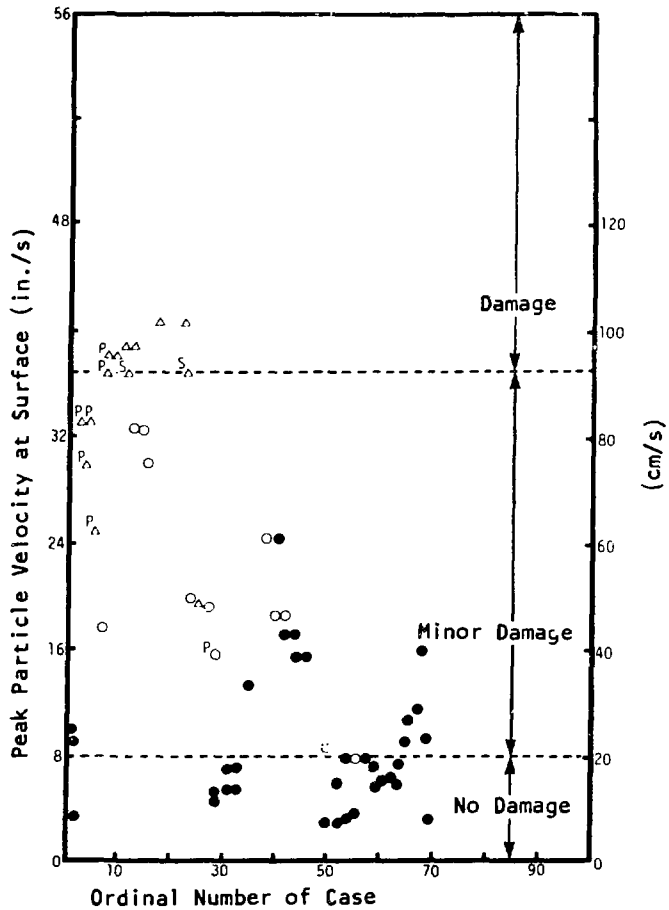

LEGEND

- ● No damage
- ○ Minor damage, due to shaking
- △ Damage from shaking
- $P_{\triangle}$ Near portal
- $S_{\triangle}$ Shallow cover

Fig. 2.2 CALCULATED PEAK SURFACE VELOCITIES AND ASSOCIATED DAMAGE OBSERVATIONS
(from Dowding and Rozan, 1978)

Thus, the authors state that surface amplification is less for low-frequency than for high-frequency disturbances. They also observed that the soil on the surface may selectively amplify certain frequencies so that the ratio of surface to underground displacement may be 10 or higher.

The oldest underground works are, of course, mines, and Stevens (1977) has compiled reports concerning the effects of earthquakes on underground mines. The many reports of earthquake shaking suggest that tunnels in solid rock perform very well under seismic shaking. However, many reports indicate that solid rock tunnels are susceptible to changes in hydrological conditions (i.e., there are reports of tunnel flooding). This would imply that, although there may have been no apparent damage to the structure, there is a probability of some shifting involving the discontinuities around the tunnels.

Stevens also cites several eyewitness accounts of seismic effects in mines. Many earthquakes that caused considerable damage on the surface were barely felt on the mining level. The type of seismic motions that did cause damage in tunnels were usually described as a roaring sound, a sharp shock, or a jolt. As examples, some excerpts are taken from the report:

> "... The first warning was a heavy roaring noise, followed almost immediately by the beginning of vibration which seemed to culminate in a very pronounced jolt, ... and for a few moments our situation was one of considerable danger and such as to leave a vivid mental impression."

> "A sharp local earthquake, reaching intensity of at least VI, ... The shock caused a staging to fall in a slope off the 4,450 foot (1,345 m) level in the Morning Mine at Mullan, ... and knocked out heading in another section of the mine ... no cave-in occurred and no ground was lost although the tremor was felt throughout the workings."

> "July 9, 1871, Kern Country, California. Severe shock felt in the Joe Walker mine, which was instantly filled with water ..."

> "... At this time, there was a great roar, people were thrown from their beds, and some were thrown to the floor ... Concrete mine foundations cracked and mine tunnels caved in..."

Ground acceleration has recently been measured in South African mines by McGarr et al. (1980) for tremors with a magnitude from -1 to 2.6 at distances from 50 m to 1.6 km. Recorded accelerations went as high as 12 g with no damage to the tunnel. This implies that factors other than acceleration, such as maximum stress and the duration of shaking, may be important for tunnel performance. Nevertheless, this study shows that underground structures are very resistant to seismic shaking, even in the near field.

Some recent and extremely interesting work involving small-scale models has been performed by Barton and Hansteen (1979). They subjected scale models of caverns (which incorporated a large number of joints) to dynamic loads. The unfavourable joint orientation and the severe pillar

design of the initial models resulted in progressive block falls and pillar collapse during the few seconds of the test. However, they state that recent tests with favourable joint geometries have shown that dynamically loaded models have suffered no block falls or collapse whatsoever despite the lack of support. This method of dynamic analysis may become a very important tool.

3. SEISMIC WAVES

3.1 BASIC RELATIONSHIPS

A sudden movement within the earth sends out seismic waves, and, when perceived by man, the phenomenon is termed an earthquake. The earthquake is the result of a loss of strength of the rock mass at the source. The movement could conceivably be elastic deformation over an arbitrary zone as a result of a sudden change in the elastic moduli of the rock. It could consist of a large number of small discontinuous movements over a volume, or the movement could occur along a planar feature, such as a fault or fault zone. Deep within the earth, it is not known exactly how the rock moves, but if a constant volume is conserved, which is most likely considering the high compressive stresses, then any shifting must exist as pure shear.

Emanating from the rapidly shearing rock mass are seismic waves that, deep within the earth, exist only as compression or shear waves. The compression wave is called the P wave (Primary wave) because it has the highest velocity and always arrives first at seismometer stations. The shear wave is referred to as the S wave (Secondary wave) and arrives after the P wave. Each has unique properties.

As the P wave travels through the rock, individual particles in its path move back and forth in a direction parallel to the line of travel of the wave (longitudinal motion). The particles in an unstressed medium also experience alternate compression and dilatation. If the rock is in a compressive stress field, then there is a changing stress resulting in an oscillation from higher compression to lower compression and back again. If the motion of the wave were to be frozen at a given instant, one would observe alternating zones of varying stress, which would move along with the wave (see Figure 3.1.1(a)).

The wave motion can be assumed to have the form of a simple sine wave. The wave, however, must be a sine wave in both space and time. That is to say, if particle displacement at a given point is plotted as a function of time (Figure 3.1.2(a)), it is a sine wave with period T. If particle displacement along the wave is plotted at a given time, the result is also a sine wave with wavelength λ (Figure 3.1.2(b)).

The particle displacement, D, at a given point as a function of time, t, may be written as:

$$D = A \sin(\omega t)$$

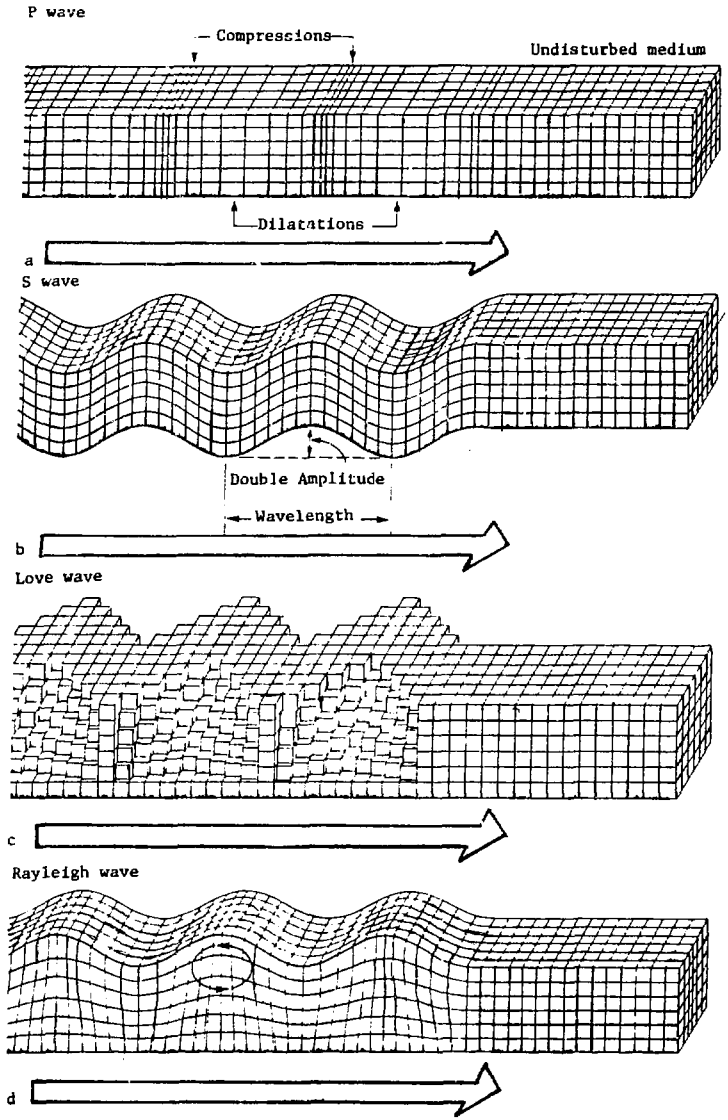

Fig. 3.1.1 MODES OF TRAVEL FOR SEISMIC WAVES
(from Bolt, 1978)

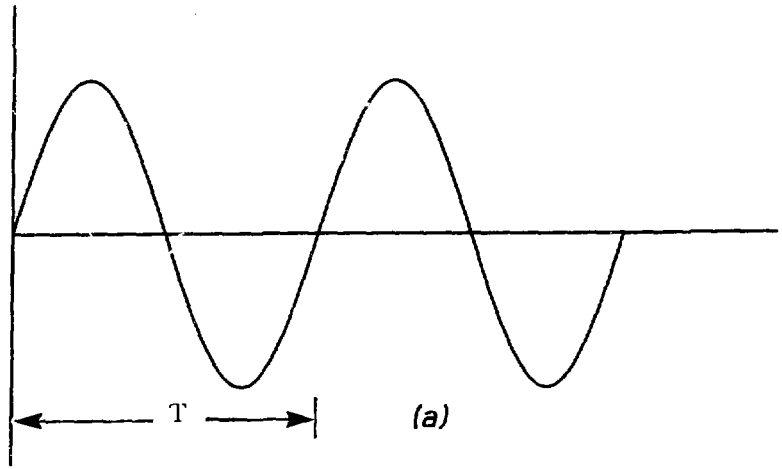

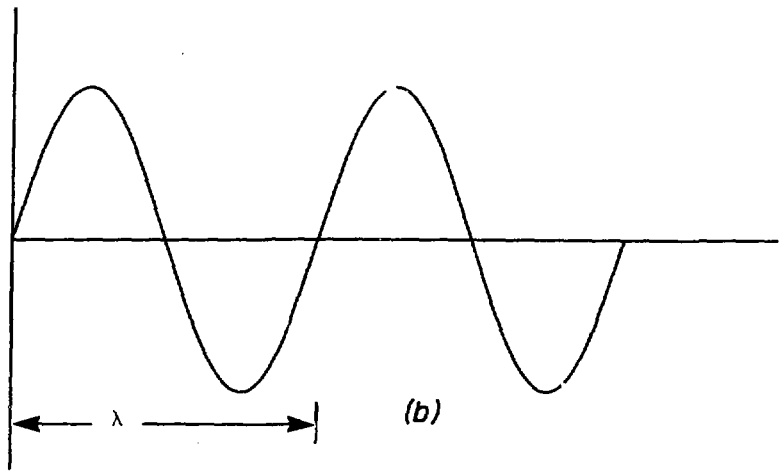

Fig. 3.1.2 PARTICLE DISPLACEMENTS IN TIME (a) AND SPACE (b)

where A is the peak displacement in metres and ω is the angular velocity, which is related to the frequency, f, by the relationship:

$$\omega = 2\pi f$$

The velocity, v, is the first time derivative of the displacement:

$$v = \dot{D} = A\omega \cos(\omega t)$$

The maximum velocity is $A\omega$ in m/s.

The acceleration, a, is the first time derivative of the velocity, or the second derivative of the displacement, and is given by:

$$a = \dot{v} = \ddot{D} = A\omega^2 \sin(\omega t)$$

Furthermore, partial derivatives can be taken in the space domain that show the interrelationship of particle displacement, stress and strain, and stress or strain gradient. A linkage can also be established between the time-varying and space-varying quantities.

Although the time-dependent equations remain the same, S waves differ from P waves in that the particles move transverse to the direction of wave travel. The rock is being exposed to pure shear stress in alternating opposite directions (Figure 3.1.1(b)). The wave velocity is slower than that for P waves, which makes the wavelength shorter for a given frequency.

The following expressions permit calculation of the stress generated by a plane seismic wave. For P waves, it is:

$$\sigma = \rho C_p v$$

and for S waves:

$$\tau = \rho C_s v$$

where σ is the normal stress in the direction of the wave, ρ is the density, C_p is the P wave velocity, v is point particle velocity, τ is the shear stress and C_s is the S wave velocity.

Differentiation leads to the equation for the stress gradient for P waves:

$$\frac{d\sigma}{dx} = \rho a$$

and for S waves:

$$\frac{d\tau}{dx} = \rho a$$

where a is the particle acceleration - longitudinal for the P wave and transverse for the S wave.

Surface waves may be generated by P and S waves striking the surface, but, once formed, they travel along the surface independently, at a velocity usually slower than that of S waves. Two types of surface waves, the Love wave and the Rayleigh wave, are shown in Figures 3.1.1(c) and 3.1.1(d).

It is not expected that surface waves could generate significant stresses at suggested disposal vault levels; certainly, high-frequency surface waves would not be expected to travel far over typically rough terrain. In this study, therefore, surface waves will not be considered, except for the fact that some observations will apply to surface waves.

3.2 LIMITS TO SEISMIC WAVES

As mentioned previously, particle displacement, velocity and acceleration, as well as stresses and stress gradients are intimately interrelated.

However, if one has only the particle acceleration-time histories for a given point, it is impossible to determine the types of waves involved or the stresses generated. Thus, horizontal motions may be due to surface waves, P waves, S waves, or one of many possible combinations of these waves in different directions. Therefore, the existing collection of acceleration -time histories from around the world does little to help quantify the full nature of seismic waves; nevertheless such records do contain useful information.

Strong-motion accelerograms have shown that horizontal peak accelerations, usually at frequencies above about 8 Hz, quite often exceed 0.5 g (Bolt and Hansen, 1977). This is generally the case when the ground motion is measured on firm ground or rock very near the source of the waves, such as for the Bear Valley, California earthquake of 1972 September 4 (M = 4.7, peak horizontal acceleration = 0.69 g); and for the Ancona earthquake of 1972 June 21 in Italy (M = 4.5, peak horizontal acceleration = 0.61 g); and particularly for the 1971 February 9 San Fernando, California earthquake (M = 6.5, peak horizontal acceleration = 1.15 g). A recent paper (Hartzell et al., 1978) also estimates that the Acapulco earthquake of 1974 October 6 (M = 5.0) produced accelerations over 1.0 g near the source. Smith et al. (1974) have calculated that earthquakes of about magnitude 2 located at a distance of about 1.5 km from an underground mine could produce accelerations of 0.1 g at the mine workings. Also, as stated previously, for near-field events, accelerations as high as 12 g have been measured in mines, without damage to the observation tunnel (McGarr et al., 1980).

These very high accelerations tend to be independent of magnitude, are associated with high frequencies, and only observed very close to the fault rupture surface. These facts are quite revealing and implications for underground structures will be examined.

For a given peak displacement, the peak particle velocity and stress increase linearly with increasing frequency. The peak acceleration

will increase with the square of the frequency. Taken in the inverse, for a given peak acceleration, the stress will decrease linearly with increasing frequency. Thus, it is possible to register very high accelerations with very little increase in stress.

Obviously, the most hazardous type of seismic wave would be one of high stress with high acceleration. For an 8-Hz P wave with an acceleration of 0.5 g, the maximum stress would be about 1.3 MPa and the peak displacement about 2 mm. A shear wave with this frequency and acceleration would produce a shear stress of about 0.9 MPa. For the same acceleration at half the frequency, the stresses would be doubled. If the frequency were doubled, the stresses would be halved. The fact that accelerations tend to increase with increasing frequency implies a stress control, i.e., some maximum allowable stress. It should be noted, however, that with a stress control there is no limit to peak acceleration, i.e., the acceleration can arbitrarily increase with increasing frequency.

Limits to stress may well be the operative mechanism of seismic waves, and if so, could be of major significance to underground structures. After all, the earthquake is generated by a finite stress change, and the rock between the source and the vault will only take a given amount of extra stress before failing, resulting in severe attenuation. It is obvious that more information is needed about the stresses associated with seismic waves.

3.3 EXPECTED SEISMIC WAVEFORMS

The previous discussion represented seismic disturbances as sine waves with a unique frequency, f. However, as seen from the seismograms in the following figures, actual seismic waves consist of a complex structure of strong motions, pulses, and trailing waves.

For a given amount of energy release, the highest accelerations and stresses will be realized if most of the seismic motion is in the form of a short pulse rather than a long wave train. These pulses are generally in records involving the highest accelerations and in those recorded close to the initiating source.

Several examples of this pulsing behaviour are:

(a) The North-South (N-S) component of the El Centro (1940) earthquake (Figue 3.3.1), which had a magnitude of 7.8 and strong motion which lasted for about 30 s. Even though this was an extremely long wave train, there were several pulses within it with high accelerations.

(b) The Parkfield (1966) California earthquake (Figure 3.3.2). This is an excellent example of a high-acceleration, pulsed earthquake. Although the peak acceleration was 0.6 g, this earthquake caused only minor damage to surface structures because of its short duration.

(c) A small magnitude (M = 1.5) earthquake near Attica, New York (Figure 3.3.3).

(d) A larger event (M = 2.2) near Blue Mountain Lake, New York (Figure 3.3.4).

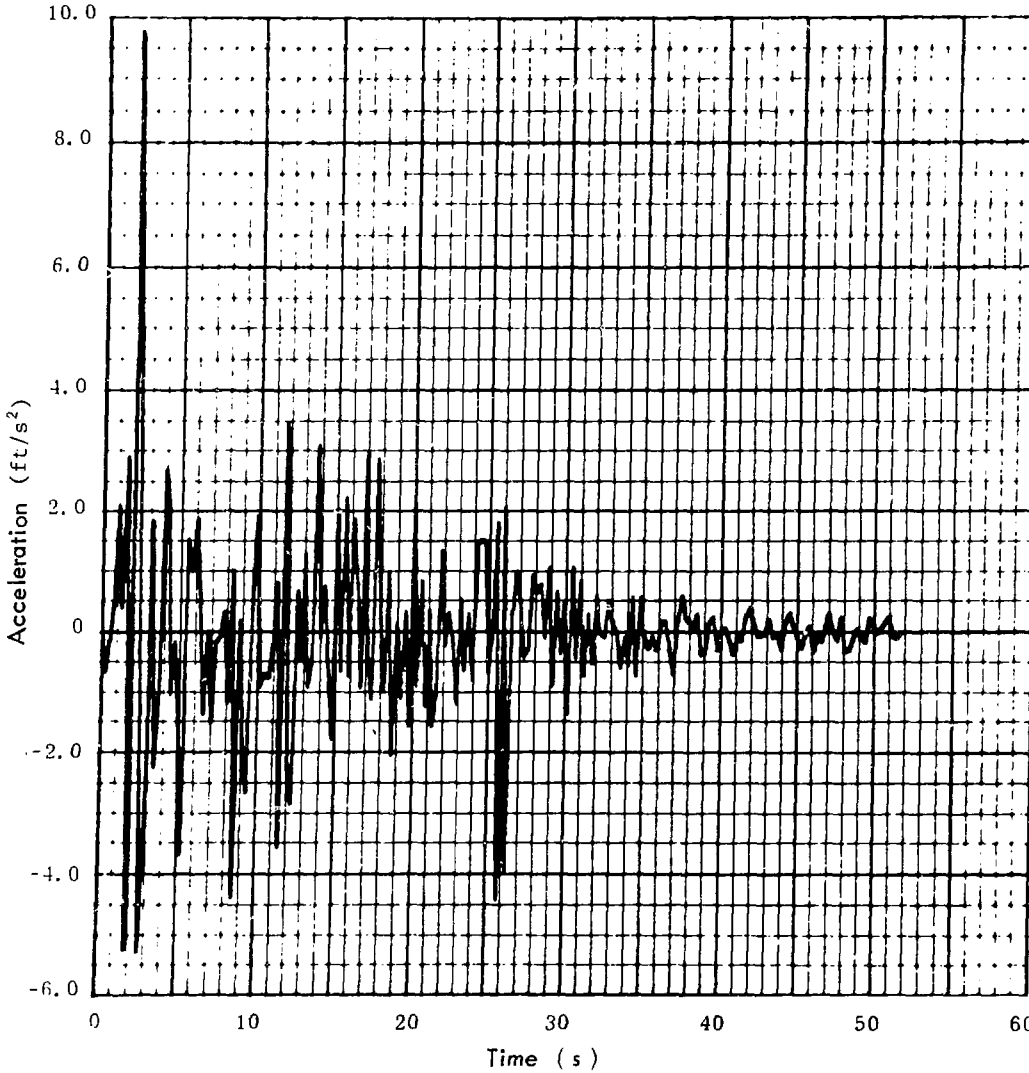

Fig. 3.3.1 N-S COMPONENT OF THE EL CENTRO (1940) EARTHQUAKE (Modified)

(from Allensworth et al., 1977)

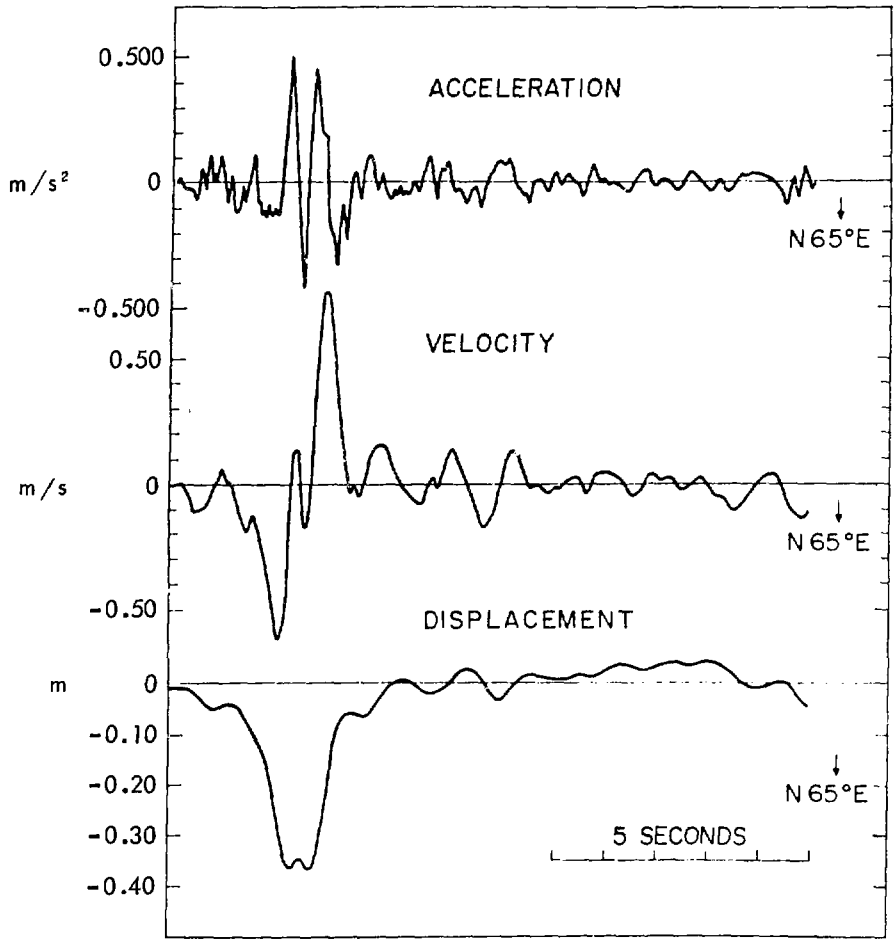

Fig. 3.3.2 PARKFIELD (1966) EARTHQUAKE
(from Aki, 1968)

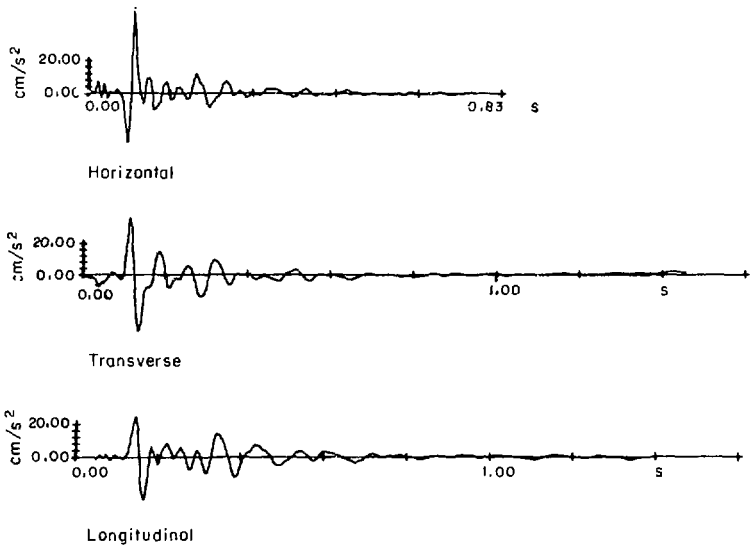

Fig. 3.3.3 THE INSTRUMENT - CORRECTED ATTICA TOTAL HORIZONTAL ACCELERATION RECORD AND THE HORIZONTAL COMPONENTS AS DIGITIZED

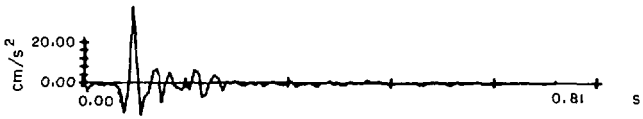

Fig. 3.3.4 BLUE MT. LAKE TRANSVERSE (EAST) ACCELERATION
(from Boatwright, 1978)

For the Parkfield earthquake, using a maximum velocity of 0.8 m/s and assuming a P wave, one obtains a calculated stress for granite of about 11 MPa. If 0.8 m/s were the maximum velocity of an S wave in an infinite medium, then the shear stress would be about 7.6 MPa. Of course, it should be remembered that these measurements were made at the surface and perhaps on materials softer than granite. Nevertheless, stresses of this magnitude could be of significance to an underground structure, and would have a high probability of causing damage.

A useful technique for analyzing these complex waveforms is Fourier analysis, whereby a recorded seismic signal can be represented as a sum of continuous sine and cosine waves of different frequencies and amplitudes. In fact, any function of time that is piece-wise smooth in the interval $-T/2 < t < T/2$ and periodic with period T may be expressed as (Kanasewich, 1975):

$$f(t) = 1/2a_o + \sum_{n=1}^{\infty} [a_n \cos(\omega_n t) + b_n \sin(\omega_n t)]$$

where

$$a_n = 2/T \int_{-T/2}^{T/2} f(t) \cos(\omega_n t)\, dt \qquad n = 1, 2, \ldots$$

$$b_n = 2/T \int_{-T/2}^{T/2} f(t) \sin(\omega_n t)\, dt \qquad n = 1, 2, \ldots$$

$$\omega_n = \frac{2\pi n}{T}$$

The amplitude spectrum of any frequency component is:

$$|F_n| = \sqrt{a_n^2 + b_n^2}$$

The phase spectrum is:

$$\phi_n = \tan^{-1}\left[\frac{b_n}{a_n}\right]$$

If the amplitude and phase for all frequencies are specified, the function is completely determined. This means, however, that it is not sufficient to specify only the amplitude spectrum for a given event. One technique for analyzing the seismic response of surface structures is to generate an artificial accelerogram from a given Fourier amplitude spectrum. There are, however, an infinite number of functions that will give the same Fourier amplitude spectrum. This is not very important for surface structures, where resonance is the chief cause of failure, but for underground structures the exact nature of the seismic motion (i.e., the phase relationships) is extremely important. Thus, it is important not to lose any information by employing only Fourier amplitude spectra.

Fourier analysis is a useful tool for many applications, but its primary use is to quantify the frequency components in a given measured history. Thus, it can be used to tell whether an acceleration-time history contains high- or low-frequency components, and to give the amplitude of these components.

3.4 GENERAL ATTENUATION

It has been seen that low-frequency waves with high accelerations will produce high stress waves, but there is a question whether these waves are realistic. The seismic wave that might reach a waste-disposal vault will be a function of the processes that created it and the processes affecting it as it travels through the surrounding rock. The chief effect of travelling through rock will be attenuation (reduction of the displacement amplitude). The specific details of how the earthquake was generated become less important the further the site is from the source; attenuation takes over as the most important factor.

To understand attenuation, consider a point source of seismic waves, such as an explosion, deep within the earth. The waves spread out and their amplitudes decrease inversely with distance. This is geometric attenuation, and is a function of source geometry and location.

When seismic waves travel through rock, however, energy is absorbed or scattered by discontinuities. Short-wavelength or high-frequency waves are most affected, due to the inhomogeneity of the rock. For lower frequencies, if the wavelengths are much longer than the discontinuities, the waves behave as though the rock were a uniform mass, with the elastic properties being an average for the various constituents.

It is still not known exactly what mechanism causes inelastic attenuation or direct energy absorption by the rock itself. It may be the movement of water in pores or the sliding of microcracks, but it is reasonable to assume that it is a direct result of the changing deviator stress or octahedral shear stress.

From observations of strong earthquakes in California and in British Columbia, Milne and Davenport (1969) developed the following expression for a, the peak ground acceleration, as a fraction of the acceleration due to gravity:

$$a/g = 0.0069e^{1.6M}/(1.1e^{1.1M} + R^2)$$

where R is the epicentral distance in kilometres, and M is the earthquake magnitude.

In eastern Canada there is apparently less attenuation, and an expression that has been used is (Basham, 1975):

$$a/g = 0.08e^{M}/r^{1.4}$$

where r is the distance to the hypocentre.

The above expressions tend to imply, although they do not necessarily assume, that the attenuation with distance is independent of the frequency of the seismic waves. Such an assumption is not realistic since it is known that, in a dissipative medium, the higher frequency waves attenuate more rapidly. Dissipation can be defined in terms of the specific energy loss, which is the ratio, $\Delta W/W$, of the amount of energy, ΔW, lost in taking a body through a stress cycle and the elastic strain energy, W, in the body at the maximum stress during that cycle (Jaeger and Cook, 1976). This can be expressed in terms of the parameter $Q = 2\ W/\Delta W$.

The geometrical and dissipative attenuation of seismic waves spreading from a point source can be determined approximately from:

$$A = (A'/r)\ e^{-\alpha(r-1)}$$

where r = the distance from the hypocentre

A' = the amplitude at unit distance from the source

A = the amplitude at the distance r from the source

and $\alpha = \pi f/QC$

where f = the frequency of the wave

C = the velocity of propagation

Q = dissipation parameter

The value of Q for the upper lithosphere is still a matter of much debate. Anderson and Hart (1978) report that it may be as low as 200, or as high as 500. Using the low value of 200, one can calculate the relative amplitudes of a 2-Hz wave and a 20-Hz wave at various distances from the source, assuming an S-wave velocity of 3000 m/s. For example, at 5 km the ratio of amplitudes for the two waves is 1.6, at 10 km it is 2.6, and at 20 km it is 6.6.

Thus, attenuation is a function of frequency for the wide range of frequencies likely to affect a cavern. This must be considered when evaluating seismic risk to a given cavern. It can be seen that a distant earthquake may generate high accelerations, but the higher frequencies will be markedly attenuated before they reach the cavern. Small events that generate primarily high-frequency waves will only be a threat if they occur in the very near vicinity.

3.5 ATTENUATION WITH DEPTH - THE EFFECT OF THE FREE SURFACE

As mentioned in the Introduction, there is some indication that there is a considerable advantage in having an installation located under-

ground during an earthquake. One reason may be because the peak acceleration decreases with depth, but this may not be the most important factor. In this discussion it is important to understand what is relevant to an underground vault, and in a discussion of attenuation with depth there are two points to be considered.

(a) Direct Comparison

Proof of attenuation with depth would be useful in comparing the seismic response of a stiff structure on the surface bedrock and the response of an underground structure, or in comparing the response at various depths, i.e., whether deeper is better. Naturally, there would be a considerable reduction in seismic amplitudes for an excavation deep in rock compared to a surface structure on soil.

(b) Bias of Existing Seismicity Data

Attenuation calculations in Canada may be biased by surface waves and soft soil deposits. Some studies may be necessary to make existing seismic risk calculations relevant for an underground vault.

These uncertainties are actually part of the much larger question as to the properties of seismic waves at depth. Some attempts to answer this question are presented below.

An underground cavern is not merely subjected to ground shaking; it is exposed to full three-dimensional travelling seismic waves. These waves can be travelling in any direction, with each wave having a unique stress pattern. At the surface it is sufficient to describe ground movement alone in the form of a time history; in an underground environment the entire dynamic stress regime must be defined.

For engineering purposes this is a problem of monumental proportions. Some simplification is in order and, as a first step, it is suggested that seismic motions be represented as single pulses. This is somewhat different from the approach of using long acceleration-time histories as input to simplified structural models. The approach here is to realize that peak accelerations occur in pulses and that the rock responds to virtually instantaneous stresses. Thus, provided that no failure is taking place, the rock cavern will have no memory of what has gone on before and will respond to the stress levels of the moment. It can be seen that by examining the response to single pulses even longer time histories can be simulated. Using the aforementioned premise of seismic motions as single pulses, many interesting aspects of seismic risk for caverns can be examined, including attenuation with depth and wave-structure interaction.

First, the field results of one of the few attempts to measure the attenuation of seismic motion with depth will be discussed, and then an explanation for these results will be put forward. Iwasaki et al. (1977) have reported results from borehole accelerometers installed at four sites

around Tokyo Bay (Figure 3.5.1). The acceleration records were obtained during 16 moderate earthquakes (M = 4.8 to 7.2) that occurred near the area from 1970 September through 1975 February.

Only one site (Kannonzaki) was in rock, which consisted of alternating layers of sandstone and siltstone. The seismometers at Kannonzaki were located at the surface and at depths of 80 and 120 m (Figure 3.5.2). Of all the events recorded, only two occurred within a distance of 100 km. Seismic waves generated by events at greater distances would have consisted mostly of surface waves, and as stated earlier only body waves are considered in this study. The two close events occurred at distances of 55 and 80 km. The plots of peak acceleration versus depth are shown in Figure 3.5.3.

The authors reported their results in terms of the surface magnification factor (ratio of the surface acceleration to the base acceleration). So, in reality, the reduction of peak acceleration with depth is not attenuation with depth, but a result of the decreasing influence of the free surface with depth. For the rock site, the authors reported an average surface magnification factor of about 1.5, although for the nearer event this factor had a value of 2.0. It will be shown that these values can be obtained by the simple mechanism of reflection at a free surface.

The field studies demonstrate that there is a reduction in seismic motion with depth, and the following discussion offers a possible mechanism for this reduction. It is sufficient, for most seismic events, to consider only the free-field wave motions, i.e., to ignore the cavern completely. Therefore, the subsequent discussion considers only an elastic half-space with no cavern.

Most previous studies in rock and soil dynamics have made the simplification that the incident seismic waves are travelling vertically upwards. This reduces the problem to one-dimensional wave propagation which can be easily solved analytically. Of particular importance is the reflection of plane seismic waves at a free surface, especially "pulse" reflection. As mentioned previously, these pulses are a common feature of near-field motions.

Reflection of a pulse at a free surface may be represented by an image wave travelling in the opposite direction. Consider a short pulse, or wavelet, with an effective frequency of 5 Hz, travelling vertically upward. It can be either a shear or compression wave (see Figure 3.5.4, where the wave shown has acceleration as its amplitude). As the wave approaches the surface, the image wave approaches from the other side. The image wave has been chosen so that as the waves meet at the surface the normal stress and the tangential shear stress are always zero. If the wave is represented graphically by its acceleration values, then the image wave will have equal acceleration values. When the waves meet at the surface, the acceleration values are added so that the accelerations are doubled at the surface, and elsewhere they are the sum of the two waves. This process continues as the waves pass through each other with the actual measurable accelerations being the sum of the two waves. Eventually, only the reflected wave is left, travelling in the opposite direction.

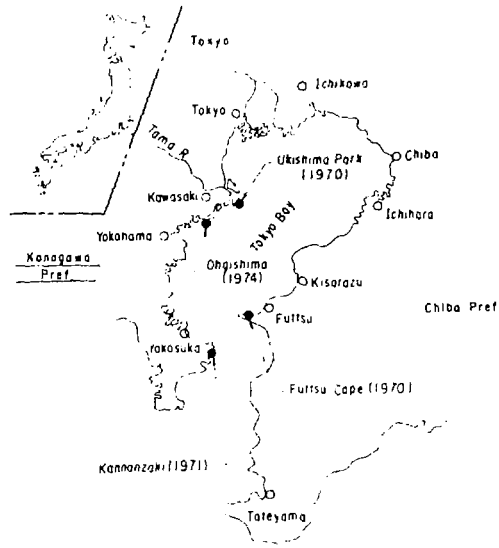

Fig. 3.5.1 BOREHOLE ACCELEROMETER STATIONS

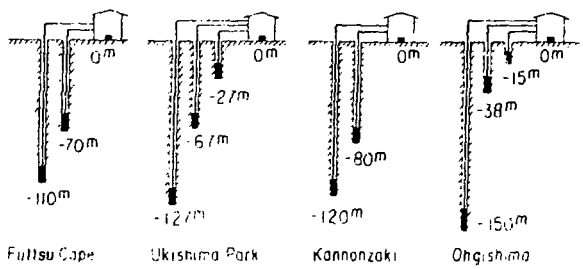

Fig. 3.5.2 DEPTHS OF ACCELERATION PICKUPS
(from Iwasaki et al., 1977)

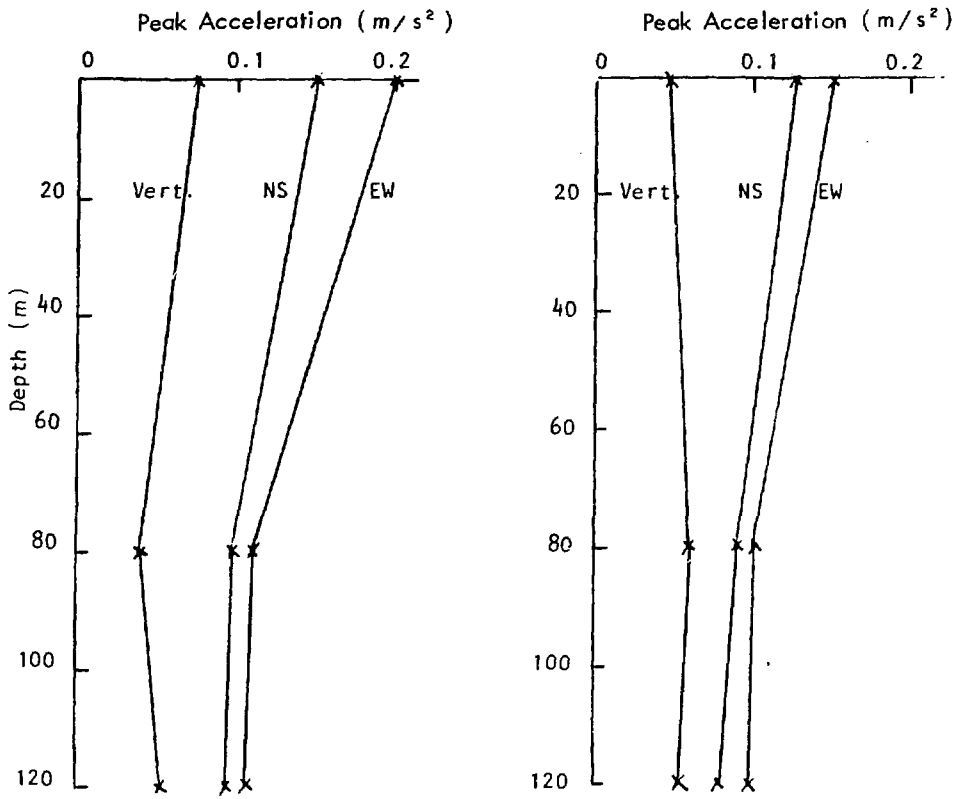

Fig. 3.5.3 VERTICAL DISTRIBUTION OF MAXIMUM ACCELERATIONS AT THE KANNONZAKI SITE
(from Iwasaki et al., 1977)

An acceleration time history measured at the surface would resemble the original wave with all acceleration values doubled. Time histories measured at various depths would be the sum of two out-of-phase waveforms, with the peak accelerations being less.

This surface-doubling effect is at a maximum at the surface and continues to decrease to a depth of about one quarter of the wavelength. Below this point there is a 50% reduction in peak acceleration. For a 5-Hz wavelet with a velocity of 200 m/s, this depth is 100 m, and for higher frequencies the depth is less.

Simple reflection can be simulated on the computer using the technique of convolution, as explained in the Appendix. The input wave is digitized so that it is defined by N discrete points with time interval Δt (Figure 3.5.5(a)). This waveform is then convoluted with a simple Dirac comb containing only two spikes (Figure 3.5.5(b)). This Dirac comb represents both the arrival of the incident wave and then the reflected wave. If the time between the first arrival of the wave at a given depth and the arrival of the reflected wave is t_R seconds, then the time gap between the two spikes is also t_R seconds, or $t_R/\Delta t$ time intervals.

The convolution of these two time series is somewhat equivalent to the method of images. The input wavelet is "folded" back on itself and is the semi-analytical representation of one-dimensional reflection at a free surface.

The waveform used in this computer study was modelled after an accelerogram obtained at Blue Mountain Lake, New York, as shown earlier (Figure 3.3.4). The simplicity and clarity of its S-wave pulse resulted from a nearly complete absence of scattering and reflections as second arrivals on the accelerogram, and a very elementary earthquake source. The effective frequency of the pulse is about 25 Hz (i.e., the best fit sinusoid).

The computer-generated time histories for various depths are presented in Figure 3.5.6. These signals are a result of a vertically incident P wave travelling at a velocity of 5000 m/s. The topmost, or surface, signal is an exact doubling of the original input wave. The subsequent signals at various depths show the gradual separation of the input and reflected waves. As these waves are separated in phase, the peak acceleration decreases. Finally, at the 450-m depth there are two distinct waves.

A plot was constructed (Figure 3.5.7) of peak acceleration versus depth for both the P wave and the S wave (C_S = 2000 m/s). The reduction with depth is not smooth because of the double-pointed shape of the input wave. A simpler pulse would attenuate more rapidly. It should be noted that the shear wave attenuates more rapidly for the same frequency simply because it has a shorter wavelength. Body shear waves are usually considered to be the more destructive to structures and internal installations, so it is a double benefit to observe that these waves attenuate more rapidly.

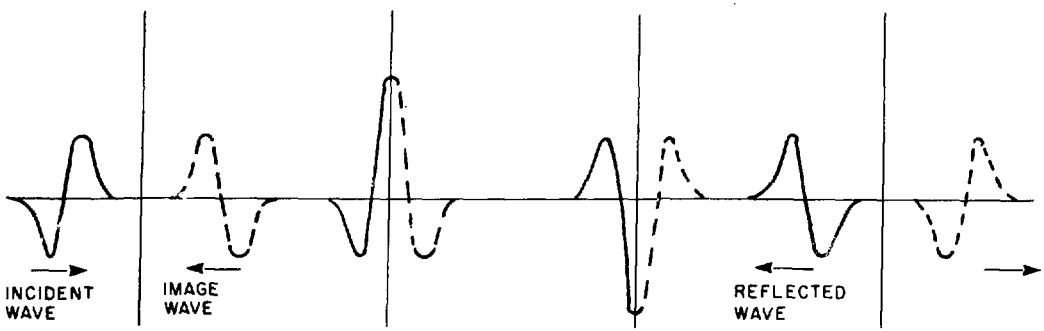

Fig. 3.5.4 REFLECTION OF A PULSE

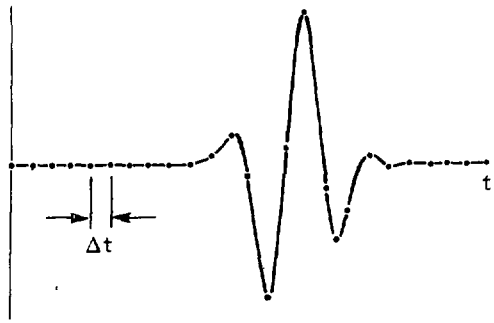

Fig. 3.5.5 (a) DIGITIZED WAVEFORM WITH SAMPLING POINTS AT INTERVAL Δt

Fig. 3.5.5 (b) DIRAC COMB WITH REFLECTION DELAY (t_R)

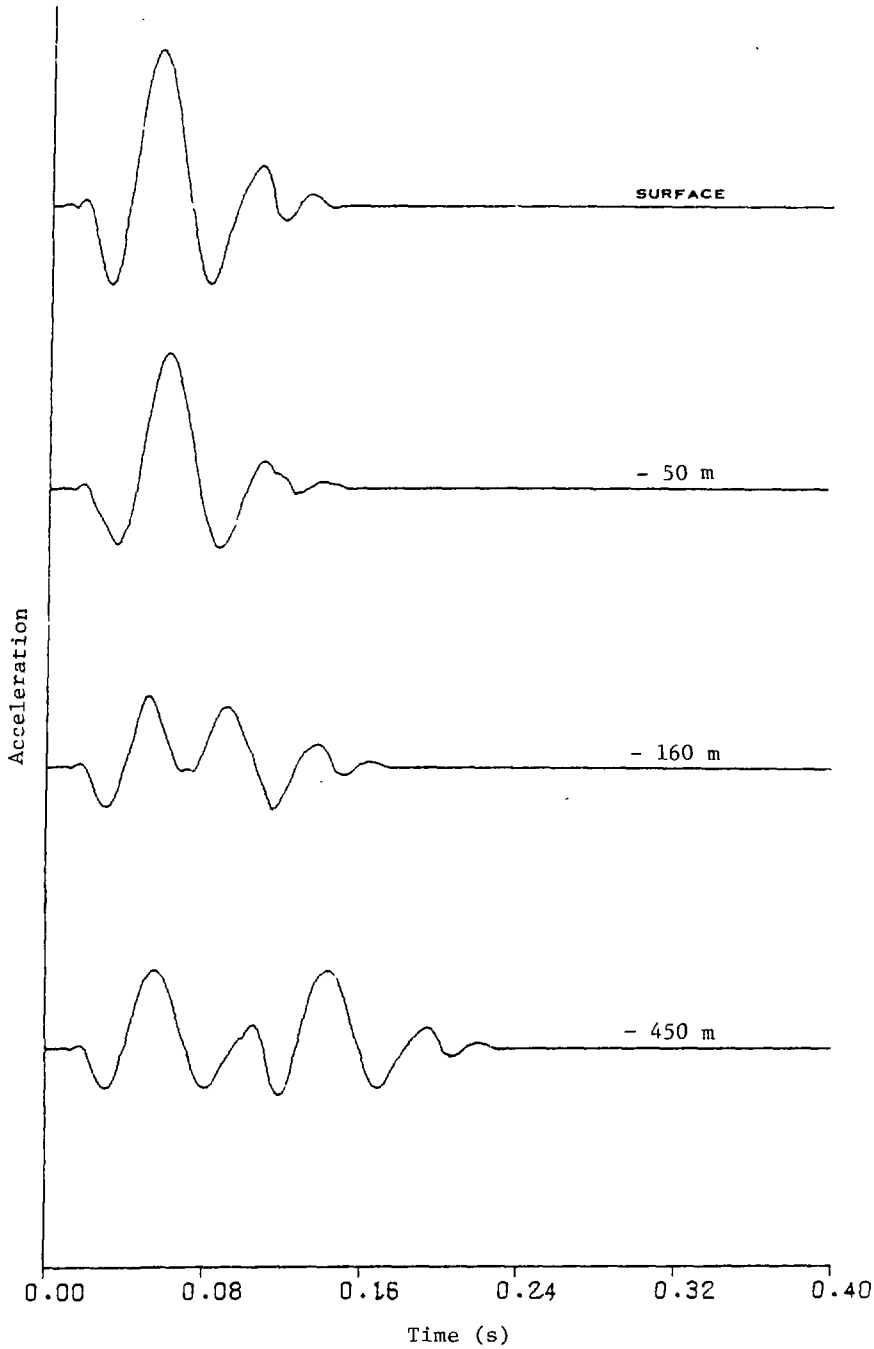

Fig. 3.5.6 CALCULATED TIME HISTORIES AT SPECIFIED DEPTHS

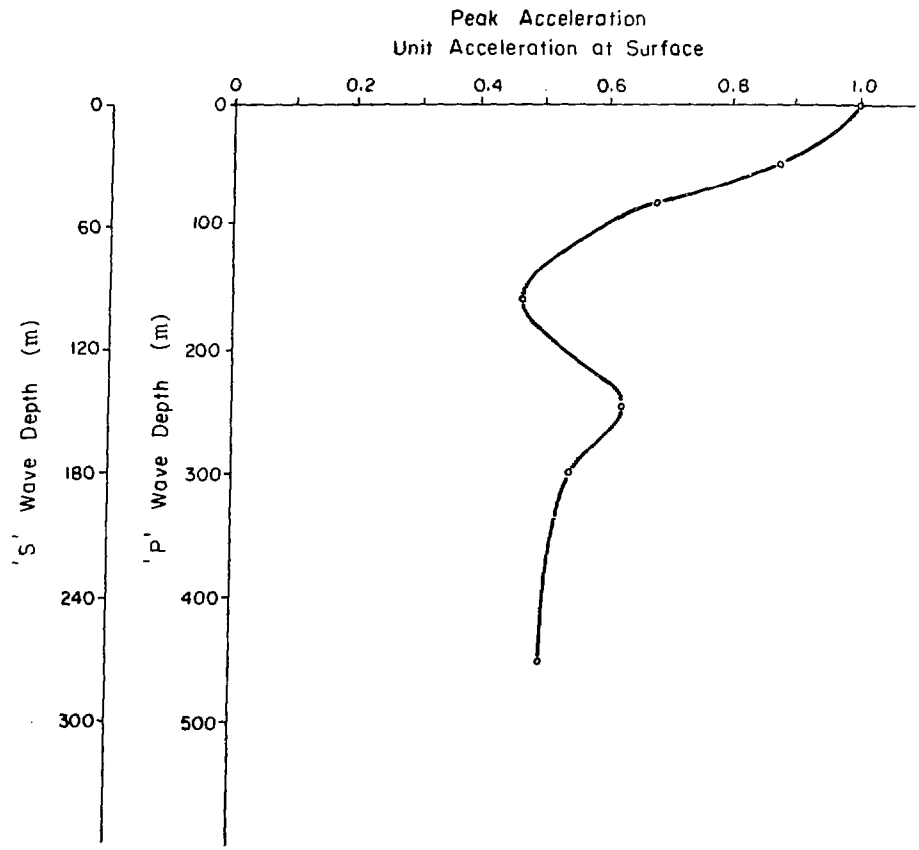

Fig. 3.5.7 PEAK ACCELERATION VERSUS DEPTH FOR 'P' AND 'S' WAVES

The time interval for the waveform can be changed to alter its predominant or effective frequency. For the 20-Hz waveform, the time interval was 0.002 s; to obtain a 10-Hz waveform, the time interval should be doubled to 0.004 s. In this way, a plot can be constructed of the attenuation factor at the 200-m depth versus the effective frequency (Figure 3.5.8). As seen, the attenuation increases with increasing frequency to about 15 Hz and does not vary in the higher frequency range. This result is a logical extension of the statement that, for each effective frequency, there is a depth at which the surface amplification ceases. This depth increases for decreasing frequency.

Vector addition of the particle motions for the incident and reflected waves suggests that the surface amplification effect will decrease for increasing angle of incidence. If the incident wave motions are vertical, then the reflected wave motions are also vertical, and the resultant of the two motions has twice the amplitude of the original wave. As the angle of incidence increases, the incident and reflected motions are no longer parallel and the resultant effect becomes progressively smaller. This is, however, a minor effect unless the wave becomes very oblique.

4. SEISMIC EFFECTS NEAR AN OPENING

Seismic waves will affect the rock in the vicinity of any underground opening by temporarily altering the surrounding stresses. However, the final excavation stresses around a deep underground excavation, such as a disposal vault, could be quite high, with certain sections of rock being in a state of near failure. This would mean that if the seismic stresses were to have any effect on the opening, it would be to trigger some failure mechanism that would be driven chiefly by the static stresses around the vault. Much like the source mechanism of the earthquake itself, most failures might be a result of frictional sliding, the mechanism discussed next.

4.1 FRICTION ALONG DISCONTINUITIES

Rock tends to behave as both a continuum and a discontinuous medium. In most cases, discontinuities control the behaviour of the rock mass as a whole. Although much effort has been devoted to studying the properties of joints and faults, there is still much to be learned. Some significant factors still requiring more investigation are: dilatant behaviour, the geometry of asperities, creep effects, strain softening, etc.

It is known that an earthquake or seismic instability cannot occur unless the resisting frictional stress decreases faster than the driving stress that is being relieved by the motion. This is demonstrated by the slider block model illustrated in Figure 4.1.1. The frictional stress (τ_f) decreases faster than the driving shear stress (τ), and the difference between the two is the stress drop ($\Delta\tau$). The decrease in (τ_f) is a direct consequence of the decrease in the coefficient of friction of the rock due to the physical mechanisms that operate when the rock moves.

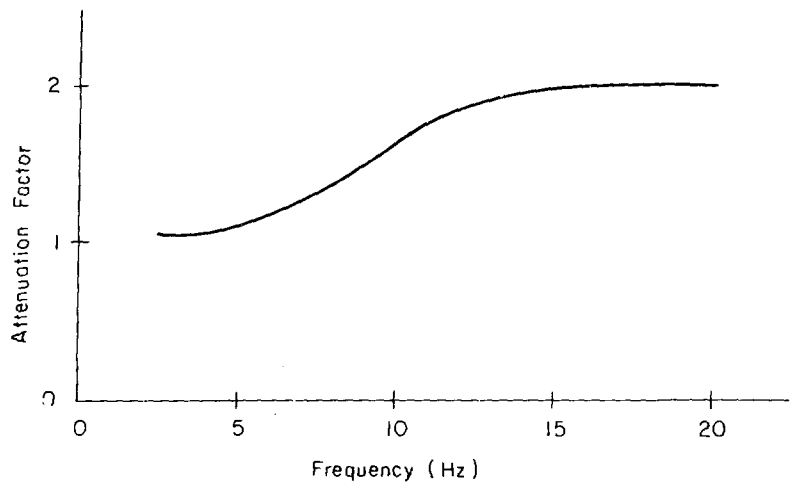

Fig. 3.5.8 ATTENUATION FACTOR vs. FREQUENCY AT 200-m DEPTH

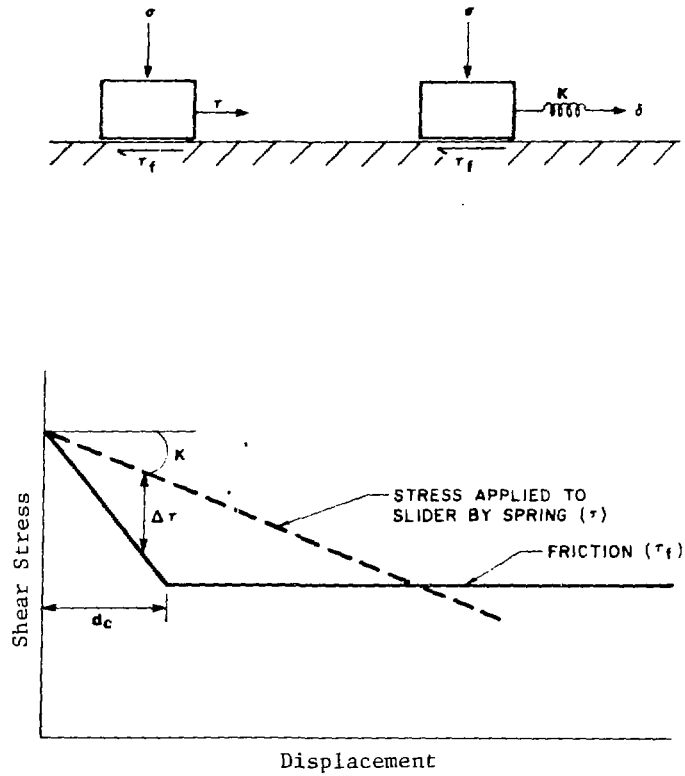

Fig. 4.1.1 SLIDER BLOCK INSTABILITY MODEL

For the purposes of analysis, a basic model of discontinuity frictional behaviour must first be developed. Once the model is functioning, the properties can be varied and refinements added. Since the exact in situ conditions are not known, it is important to perform parametric analysis using a computer model to assess the significance of variations.

As a starting point, it can be assumed that the frictional properties of rocks, like those of metals and most other materials, are largely controlled by adhesion at actual points of contact between sliding surfaces, or between gouge particles separating the surfaces (Dieterich, 1978 and 1979). It is not necessary that adhesion be the only mechanism, but it does provide the elements necessary to explain the "worst case" of seismic instability.

Bowden and Tabor (1964) proposed that when two surfaces are brought together there cannot be complete contact because of minute surface irregularities. Actual rock-to-rock contact is limited to scattered points (asperities), even for flat, well-polished surfaces. An increase in the normal stress pushing the surfaces together causes the contact points to yield and results in an increase in the actual area of contact. For a unit area of surface, the actual area of contact (A) may be approximated by:

$$A = C\sigma$$

where σ is the average normal stress applied over the entire surface (assuming 100% contact) and C is a material constant inversely proportional to the indentation hardness or yield stress. Bowden and Tabor assert that the resistance of the surface to slip is controlled by the adhesive strength of the junctions. It follows that the average uniform shear stress required for slip to occur is proportional to the real area of contact:

$$\tau = FA$$

where F is the strength per unit area of a contact. The coefficient of friction, μ, is given by

$$\mu = \tau/\sigma = CF$$

Note that CF is dimensionless and that the shear stresses at points of contact are independent of the applied normal stress.

It has been shown by several researchers (Dieterich, 1972; Scholz et al., 1972; Teufel and Logan, 1978) that friction is dependent on time, velocity and displacement. In general, the coefficient of friction increases with the time of stationary contact and decreases with increasing velocity. The empirical law proposed by Dieterich (1978) for time dependence is:

$$\mu = \mu_o + A \log (Bt + 1) \qquad (1)$$

where μ is the coefficient of friction given by the ratio of shear stress to normal stress, τ/σ, t is the time of contact measured in seconds, and μ_o, A, and B are constants with values of approximately 0.6-0.8, 0.01-0.02, and

1.0-2.0, respectively. The measurement of sliding friction at different velocities of slip (Dieterich, 1978) has shown an analogous velocity dependency:

$$\mu = \mu_o + A \log [B(d_c/\dot{\delta}) + 1] \qquad (2)$$

where d_c is an experimental parameter and $\dot{\delta}$ is the slip velocity. Note that Equation (2) is identical to Equation (1) if the constants μ_o, A, and B are the same and time t is replaced by:

$$t = d_c/\dot{\delta} \qquad (3)$$

Displacements and velocities are in centimetres and centimetres per second, respectively. The parameter d_c represents a displacement dependence for the coefficient of friction, i.e., it does not drop immediately upon movement but only after a critical displacement, d_c. This parameter, which is independent of normal stress, has very small values of about 5×10^{-4} cm and 1×10^{-10} cm for surfaces lapped with No. 240 and No. 600 abrasives, respectively (Dieterich, 1978). The value of d_c is not known for joints and would need to be measured in a laboratory programme.

The physical meaning of these parameters has been explained by Dieterich (1978). He states that t in Equation (3) is the average lifetime of a population of adhesion contacts, and that d_c is the displacement required to change the population of contact points completely. Going back to the adhesion model discussed earlier, it can be seen that as a joint begins to move old adhesion contacts are being broken and new ones are being made. After a displacement of magnitude d_c, all the old contacts have been broken. The strength of the new contacts is a function of time, and if they are being broken in short order, the overall coefficient of friction is reduced. This is the state of dynamic sliding friction

The stability of a mechanical system (such as joints in a rock cavern) will depend on the magnitude of the stress drop and how rapidly the stress drop occurs. Acceleration of the sliding occurs when the frictional resisting stress decreases faster than the elastic stress forcing the motion. It follows that the faster the stress drop, the faster the acceleration. Factors favouring unstable slip are: low stiffness, high normal stress and small d_c. Similarly, large contact times combined with high loading velocities favour instability, due to the fact that there would be a high initial shear stress followed by a rapid stress drop. It has also been shown that a block experiencing stable slip can be induced to slide unstably if a perturbation that increases slip velocity results in a rapid decrease in friction.

To relate these observations to a disposal vault or other underground facility, the factors that favour instability are: high stresses, the possibility of smooth joints that have been stationary for a long time, and the brittleness of the rock. Factors that favour stability are: high stiffness of the rock, and the confinement of joint blocks due to the relatively small size of the postulated caverns.

With reference to seismically induced instability, it should be noted that a rapid increase in relative or differential velocity contributes to instability. Also, joints blocks that are in a state of stable sliding may be accelerated by seismic motion and put into a state of unstable slip. Dieterich's work (1979) also suggests that joints resist rapid relative velocity changes, which would make it more difficult for a short duration seismic event to initiate sliding.

Of course, none of these mechanisms will operate if the discontinuity is not already stressed very close to failure. Rapid failure, such as a rock burst, may occur spontaneously without seismic waves acting as a trigger, or slip may occur during excavation, or stress relief may occur slowly. Whether or not seismic stresses are important depends entirely on how near to failure a discontinuity can exist without some movement occurring.

4.2 POSSIBLE FAILURE MECHANISMS

Several rock failure mechanisms could be triggered by earthquakes, or occur spontaneously. Although there may be others, the three with the highest probability of occurrence are slabbing, joint block movement (rock blocks falling), and joint shifting (joint or fault slippage), as illustrated in Figure 4.2.1.

Slabbing may occur if the rock is previously weakened, and is affected by perpendicular wave action as mentioned previously. Its susceptibility to triggering by earthquakes is dependent on how close to the cavern surface the seismic stresses can penetrate. Accelerations alone would have a small effect on thin slabs because of their low mass. Thus, slabbing could most likely only be caused by high-frequency, high-stress waves, which, as mentioned earlier, would be extremely rare and would be quite destructive in other ways if they did occur.

The falling of rock blocks follows some of the same rules as slabbing. It will be sensitive to stress changes near the surfaces of the cavern and the associated accelerations. The worst case would occur if the confining pressure were reduced on a block accelerating into the cavern. The stability of rock blocks, however, is an extremely complicated question because it involves movement along several planes in three dimensions, and will not be extensively discussed in this report. It is the author's opinion, though, that it would be very difficult for seismic waves to loosen rock blocks because such a block is normally well confined, and the accelerations can only act by effectively increasing the weight of a block for a short time. The larger the block, the larger the confining area. The effect of an earthquake, therefore, is almost the same as attaching a rock bolt to the block and pulling rapidly with some fraction of its weight. It is not expected that, in any well-constructed underground cavern, rock blocks would shift due to such treatment.

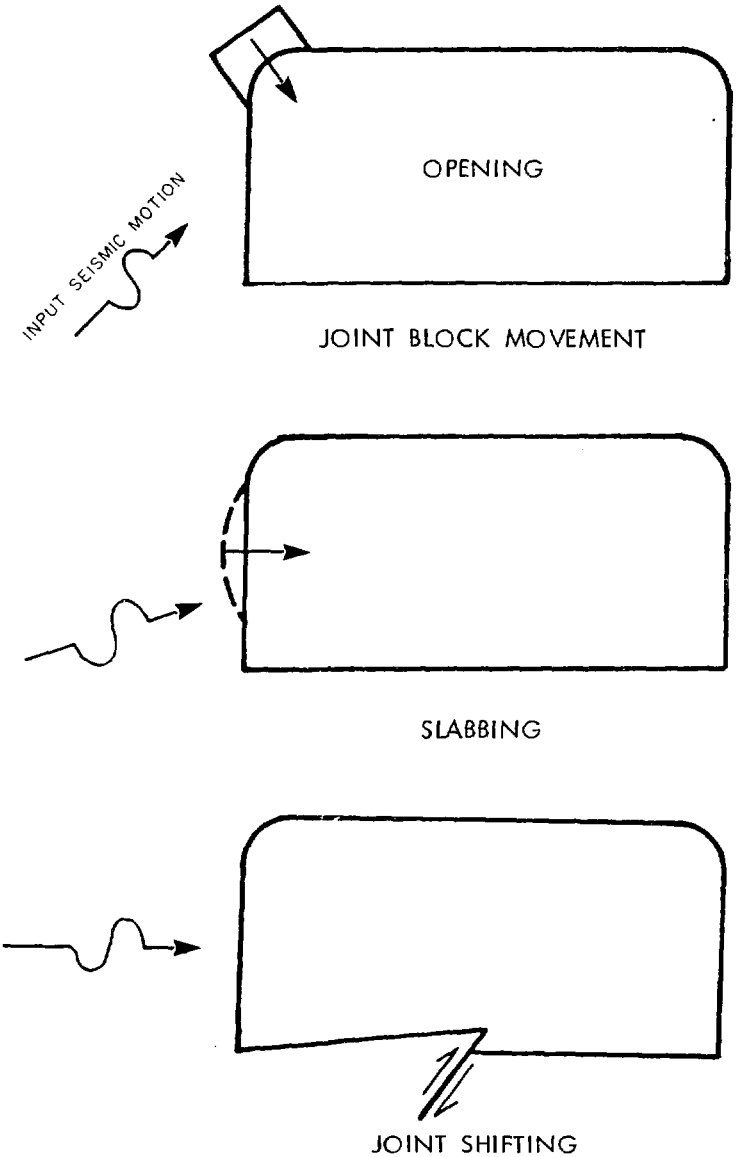

Fig. 4.2.1 POSSIBLE FAILURE MECHANISMS

The most significant failure mechanism, and the one on which this study concentrates, is dynamic shifting along discontinuities. This would be especially significant if it occurred through waste canisters in a vault floor, and should be considered when locating a disposal vault. It would, in fact, be significant if it occurred anywhere near the cavern complex because the seismic waves generated would probably trigger some of the less likely failure mechanisms.

5. COMPUTER ANALYSIS

There is obviously a need to study the mechanics of seismic wave interaction with rock. After much consideration, the method chosen was a central finite-difference code. This approach has several advantages, namely:

(a) The grid is interlaced in both space and time, giving second-order accuracy with first-order simplicity.

(b) Non-linear properties can be included by direct calculation of the relevant parameters at one instant in time.

(c) The method is relatively inexpensive.

This computer code virtually forces a detailed look at the mechanics of small sections of rock, i.e., causes of damping, effect of tension, failure modes, and dynamic effects.

It should be remembered that since the input parameters for dynamic stability are not well defined the main purpose of this numerical modelling is to show general principles and to demonstrate the potential of computer analysis. The method is sufficiently flexible that joints with non-linear properties can be introduced in order to more accurately model the behaviour of a real rock mass.

5.1 CENTRAL FINITE-DIFFERENCE METHOD

The central finite-difference method for elastic solids is somewhat similar to the finite-element method, in that the solid is represented by discrete blocks. However, the finite-difference method used here is an explicit formulation rather than an implicit formulation, as used in the finite-element method. An explicit method does not simultaneously solve the equations of the whole system. It relies on the fact that the time-step increment is so small that any movement at one node only affects the adjacent node. An implicit procedure solves simultaneously for the entire system.

The equations of motion for seismic waves in an elastic solid are (Prater and Wieland, 1976):

$$\rho\ddot{u}_i + Ku_i = T_i \qquad (1)$$

$$T_i = \sigma_{ij,j} + b_i$$

where ρ is the density, K is the damping factor, σ_{ij} is the stress tensor, b_i represents the body forces, and u_i represents the displacements.

The body forces, b_i, are constant throughout the problem, and for that reason can be set to zero for wave propagation (Jaeger and Cook, 1976). However, the body forces cannot be ignored when considering discrete joint block movement.

The strain-displacement law is:

$$\varepsilon_{ij} = 1/2\ (u_{i,j} + u_{j,i}) \qquad (2)$$

where ε_{ij} is the strain tensor.

If the material is elastic, there is a unique stress-strain relationship:

$$\sigma_{ij} = C_{ijkl}\varepsilon_{kl} \qquad (3)$$

where C_{ijkl} is a tensor of all possible elastic constants.

For this analysis, we assume plane strain conditons, i.e., standard two-dimensional analysis. Assuming also that the material is homogeneous and isotropic, then, in Cartesian coordinates, Equations (2) and (3) reduce to:

$$\sigma_{xx} = (\lambda + 2G)\frac{\partial u_x}{\partial x} + \lambda\frac{\partial u_y}{\partial y}$$

$$\sigma_{yy} = \frac{\lambda\partial u_x}{\partial x} + (\lambda + 2G)\frac{\partial u_y}{\partial y} \qquad (4)$$

$$\tau_{xy} = G\left(\frac{\partial u_x}{\partial y} + \frac{\partial u_y}{\partial x}\right)$$

where λ and G are the Lamé constants.

Equations (1) and (4) can be used together to give the complete solution for wave propagation. In particular, it is better to use velocity, v_i, as the working variable in Equation (1), to produce first-order equations that are easy to formulate, i.e.,

$$\rho v_i = T_i$$

$$T_i = \sigma_{ij,j} \qquad (5)$$

These equations, together with the boundary conditions, completely define the problem.

The central finite-difference formulation employs four superimposed and interlacing grids. One grid is used for each of: the normal stresses σ_{xx}, σ_{yy}; the shear stress τ_{xy}; the x-displacements ($u_{m,n}$); and the y-displacements ($v_{m,n}$). Note that m,n now represent locations in the finite-difference grid. The complete grid is shown in Figure 5.1.1. This interlacing grid method simplifies the central finite-difference equations.

The equations of motion (4) become, in the central finite-difference formulation (temporarily eliminating the damping terms for simplicity):

$$\rho/\Delta t \ (\dot{u}_i^{t+1} - \dot{u}_i^{t})_{m,n} = (T_i^{t+1/2})_{m,n}$$

which can be rewritten as:

$$(\dot{u}_i^{t+1})_{m,n} = \Delta t/\rho \ (T_i^{t+1/2})_{m,n} + (\dot{u}_i^{t})_{m,n}$$

The displacements are calculated using simple single-order integration:

$$u_i^{t+3/2} = u_i^{t+1/2} + \Delta t \ \dot{u}_i^{t+1}$$

The whole procedure is conditionally stable since this is an explicit formulation. To ensure stability, Δt must be kept small, according to the condition:

$$\Delta t < \left\{ \frac{\rho}{\lambda + 2\mu} \ \frac{1}{\left[\left(\frac{1}{\Delta x}\right)^2 + \left(\frac{1}{\Delta y}\right)^2\right]} \right\}^{1/2}$$

Establishing a proper damping relationship is essential for the central finite-difference method, which tends to generate very high frequency waves. Two methods of damping were chosen: absolute motion damping and differential motion damping.

The absolute motion damping used is the same as that used by Prater and Wieland (1976) and is introduced through the term K in Equation (1); in the computer program, however, it is added as a separate force term calculated from the point velocity. It can be seen that the viscous damping is related to the velocity of a particle relative to the stationary frame of reference. It helps to damp out some waves, but is not related to an actual physical process.

The more natural approach would be to make the damping dependent on the relative velocity between adjacent particles. Such a mechanism would

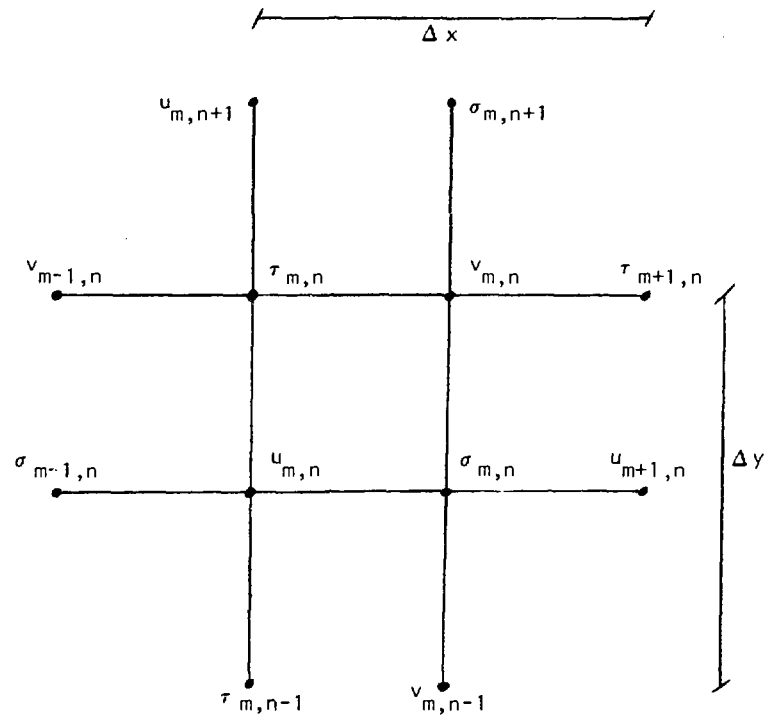

Fig. 5.1.1 SYSTEM OF INTERLACING NETS FOR FINITE-DIFFERENCE GRID

be comparable to hysteresis in rock, or damping due to the movement of water in pores, or perhaps the frictional sliding of microcracks. There may be more realistic damping models, but this method, at least, has the advantage of being able to damp out high-frequency, high-acceleration waves quite rapidly, much as real rock can. As before, it is added as a separate force term, derived from the difference in velocity between adjacent node points.

5.2 BOUNDARY CONDITIONS

A free boundary has zero normal stress and zero tangential stress. Provided these conditions are continuously met along a boundary in the computer model, it will behave as a free surface when reflecting seismic waves. This is the type of boundary used for the cavern sides.

The other type of boundary employed along the outer edges of the model is a combination transmitting and absorbing boundary. Although the medium being modelled extends for a considerable distance beyond the opening, the computer model is confined and has boundaries that reflect seismic waves. These boundaries must also input seismic motions in a manner analogous to a plane wave passing through the cavern area at an arbitrary angle. Absorption is accomplished by using the viscous boundaries devised by Lysmer and Kuhlemeyer (1969), whereby energy is absorbed at the boundaries simulating the continuous wave propagation of an infinite medium. This special type of boundary only functions if the incident wave impinges on the boundary at an angle greater than about 40 degrees, i.e., not at grazing incidence.

On these boundaries, the surface stresses are set on the positive x face according to the following formulas:

$$\sigma_{yy} = -a\rho C_p \dot{u}_x$$

$$\tau_{xy} = -b\rho C_s \dot{u}_y$$

where C_p is the P-wave velocity, C_s is the S-wave velocity, and a and b are constants that for most purposes can be set equal to one. On the positive y face, the formulas are:

$$\sigma_{yy} = -a\rho C_p \dot{u}_y$$

$$\tau_{xy} = -b\rho C_s \dot{u}_x$$

For the negative x and y faces, the signs are reversed.

The seismic input is accomplished by calculating the expected velocities for a plane seismic wave along the transmitting boundaries and subtracting these velocities from the actual boundary velocities used in the absorbing boundary equations.

5.3 APPLYING FAULT MECHANICS

The fault, or discontinuity, is modelled as a linear chain of grid points that may be one to two grid points thick. The locations of these points are stored, and are constantly monitored throughout the computer run. At each time step the normal and shear stresses are calculated and, if the shear stress exceeds the maximum allowable stress, the element is allowed to "slip" in order to reduce the shear stress to the maximum permissible value.

Slippage is implemented by storing the values of movement in a special array, and then by subtracting the associated strain from the strain values for the fault grid points so that the strains and stresses along the fault do not become excessively large.

The choice of dynamic friction parameters is most important in controlling the stability of a discontinuity. As the purpose of this study was to develop a methodology for studying dynamic response, it was decided that several orientations of faults would be chosen, and the significance of several of the following parameters studied.

The first parameter is the commonly known static coefficient of friction, μ. If this is very high, the discontinuity will never fail. A low value would most likely mean that the discontinuity had shifted and relieved the stress while the cavern was being excavated.

The dynamic coefficient of friction was made to follow roughly the guidelines stated by Dieterich (1979). Reduction only occurs if a critical displacement has occurred; the reduction is dependent on the log of the differential velocity. The reduction can only drop to a specified minimum, although it is possible that the coefficient of friction could go to zero (Sibson, 1977) if conditions are right. An instantaneous drop to zero would, of course, be the most catastrophic event that could happen to a discontinuity.

5.4 INITIAL WAVE TEST

Before a detailed tunnel model was set up, it was decided to test the finite-difference grid by passing seismic waves through it and observing reflection from a free surface. This resembles the situation discussed earlier of a seismic pulse reflecting from a wall, but this time we use inclined waves.

The cavern wall is once again modelled as the vertical free surface of an elastic half-space and forms one boundary of the finite-difference grid. The other sides should extend to infinity, but as this is not numerically possible, absorbent/transmitting boundaries form the other three sides. The model, therefore, consists of a square with one free-surface boundary and three absorbent boundaries (see Figure 5.4.1). This is a two-dimensional representation of a three-dimensional prohlem, so the plane strain asumption holds.

The P wave is generated in the lower left-hand corner of the grid system and aimed for the upper right-hand corner. It is generated by speci-

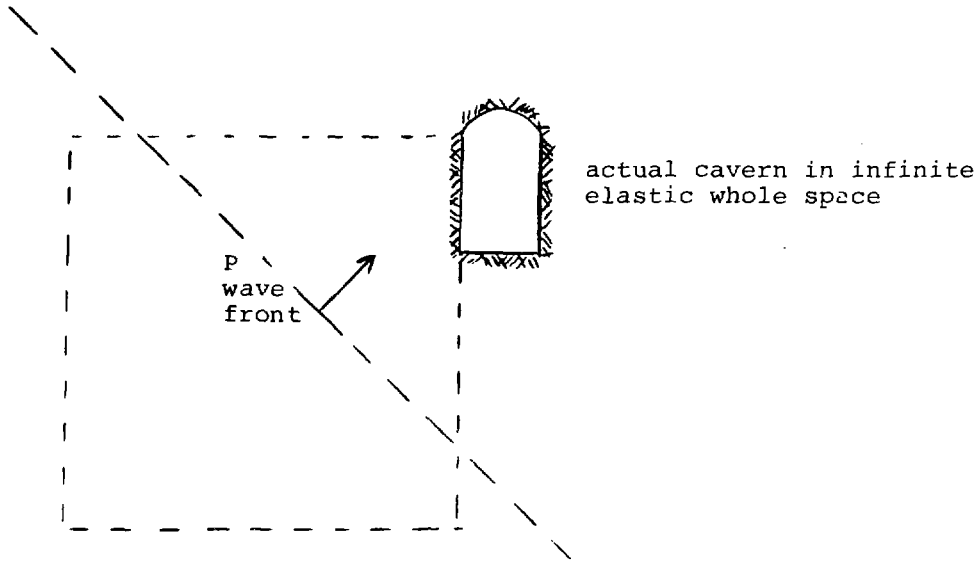

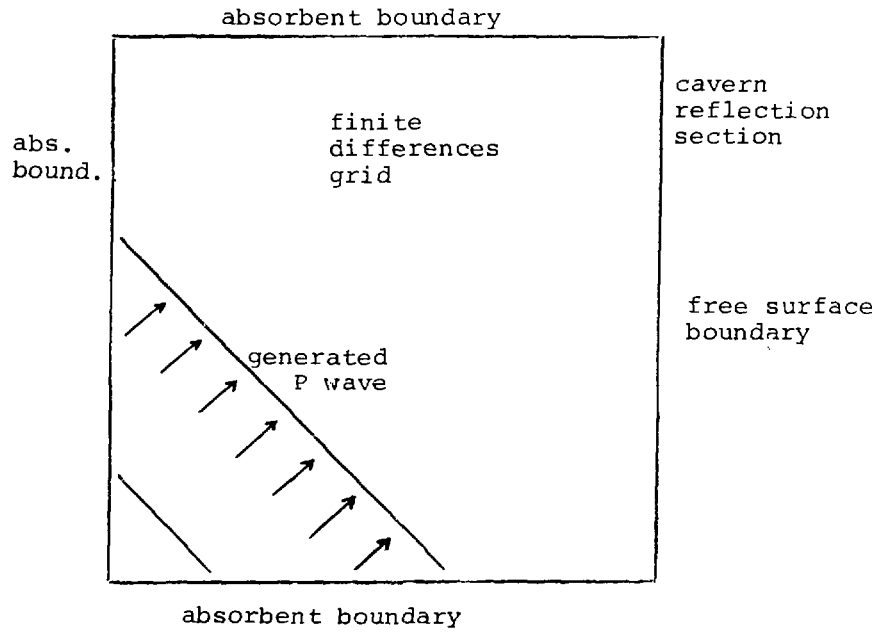

Fig. 5.4.1 INITIAL WAVE TEST MODEL

fying the velocities as a triangular distribution on a band of grid points, which is perpendicular to the direction of travel. This method of generation proved quite suitable for this type of wave as it produced a pulse that closely resembled real pulse earthquakes, as discussed in a previous section. Unfortunately, the wavelength and, therefore, the frequency of the wave were limited by the size of the grid. Furthermore, S waves generated by this method suffered extensive interference from the leading P waves, as shall be seen in the computer results.

Once the P wave has been generated, it travels to the free surface and is reflected. It should be noticed that the P wave strikes only the upper portion of the free surface, and it is here where measurements are made. Thus, if the grid spacings are 5 m and the grid is a 40 x 40 matrix, then the dimensions of the main finite-difference grid is 200 m x 200 m, but the actual tunnel wall can be taken to be a small section in the upper part of the free surface. There may be an objection, then, that the majority of the free surface should be modelled as an absorbent boundary as it is representing an unbounded medium. But it should be remembered that any wave energy reflecting off the lower portion of the free surface will be directed away from the area of interest.

As a check on program performance, waves were generated and reflected from the free surface. "Snapshots" of these waves were created by taking the curves of velocities through the grid points and then shading only the positive portions. The pictures (Figure 5.4.2) were created by using the x-component of velocity. The P wave propagates as it should and reflects at the correct angle. The shear wave presents a problem, however. It is preceded by a small P-wave pulse created during initialization. After this wave passes, however, what remains is pure S wave. It also reflects in the classical manner.

The wave used for the detailed studies had an effective frequency of about 55 Hz, which is quite high, but the results can be generally applied to lower frequencies. Lower frequencies could only be obtained at greater expense, as there must be a trade-off between better resolution and a larger total grid. That is to say, for a given matrix size, a larger grid could be obtained by increasing the spacing between grid points, but this would mean poorer resolution. As it was, the computer program used a 40 x 40 matrix with a 5-m spacing between grid points, which for some purposes may still be too large. It should be remembered that a 40 x 40 matrix has 1600 main grid points, or 6400 staggered grid points, and uses a large amount of computer memory. A larger matrix would use more memory and computer time.

The pulse used for the detailed studies was a 45-degree P wave with an effective acceleration frequency of about 55 Hz. The values of velocity, acceleration, displacement and stress were recorded as a function of time at receiver sites at various distances from the wall. These were plotted using a GOULD electrostatic plotter and are shown in Figures 5.4.3, 5.4.4, and 5.4.5.

Because the grid points are 5 m apart, the surface receiver gives the best indication of near-surface block behaviour. On these plots, tension is positive, which is common in elasto-dynamics, but is the opposite of

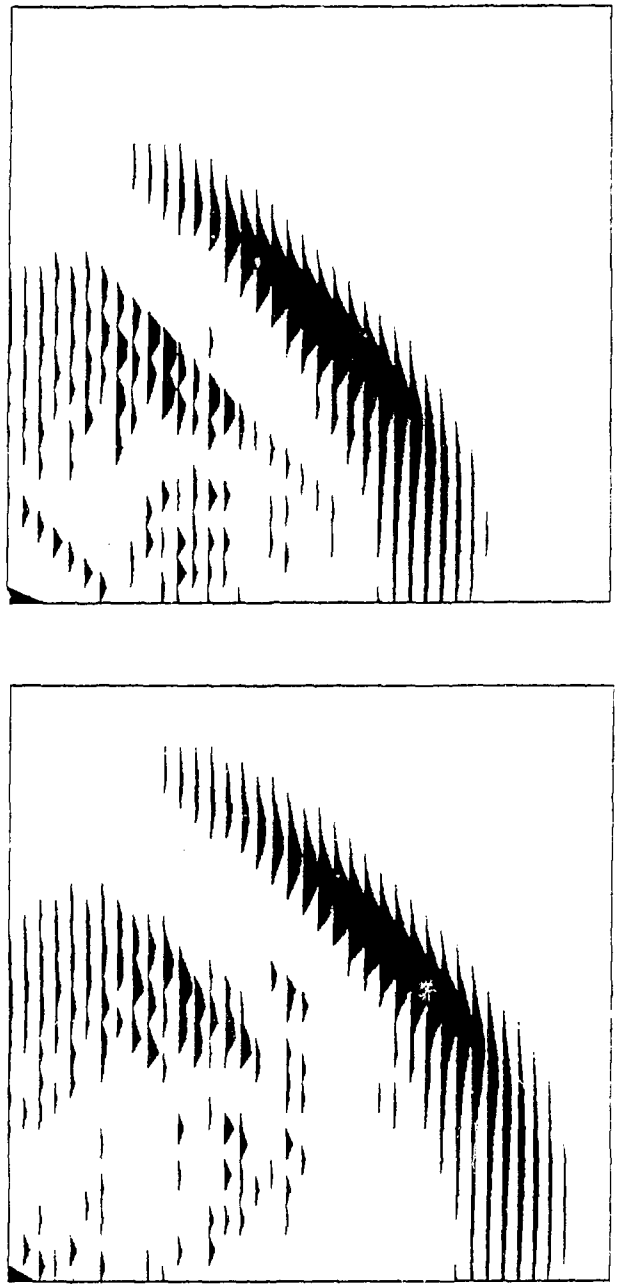

Fig. 5.4.2 (a) PROPAGATING P WAVE IN FINITE-DIFFERENCE GRID. WAVE ORIGINATED IN LOWER LEFT CORNER.

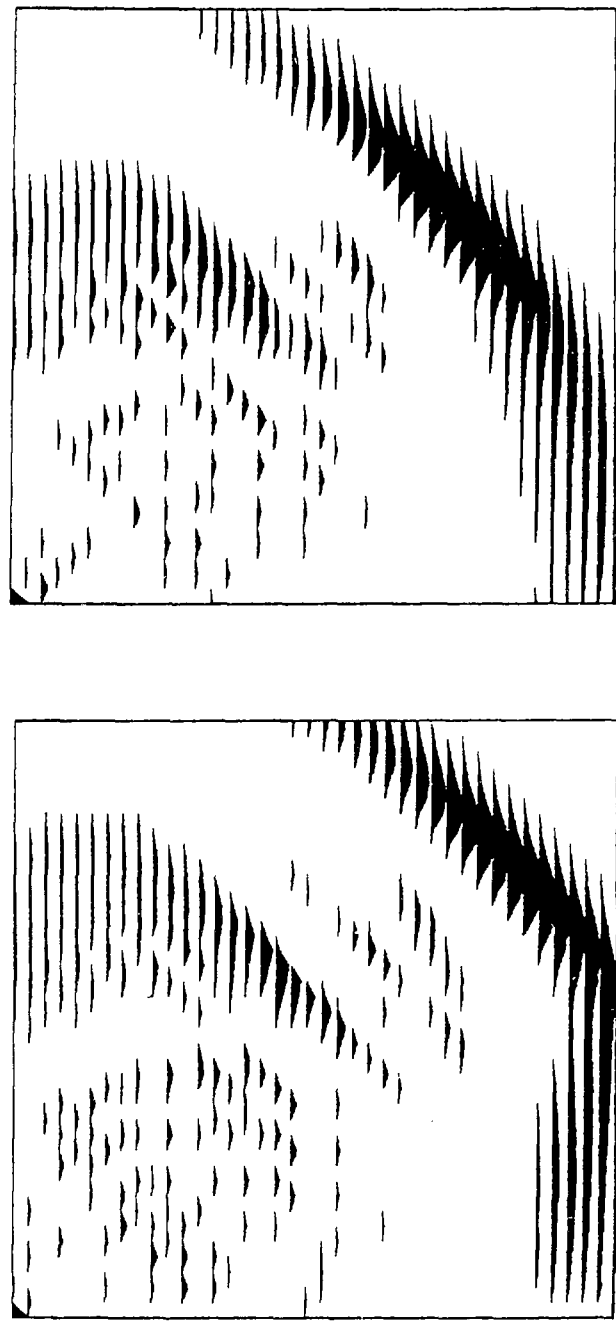

Fig. 5.4.2 (a) CONTINUED

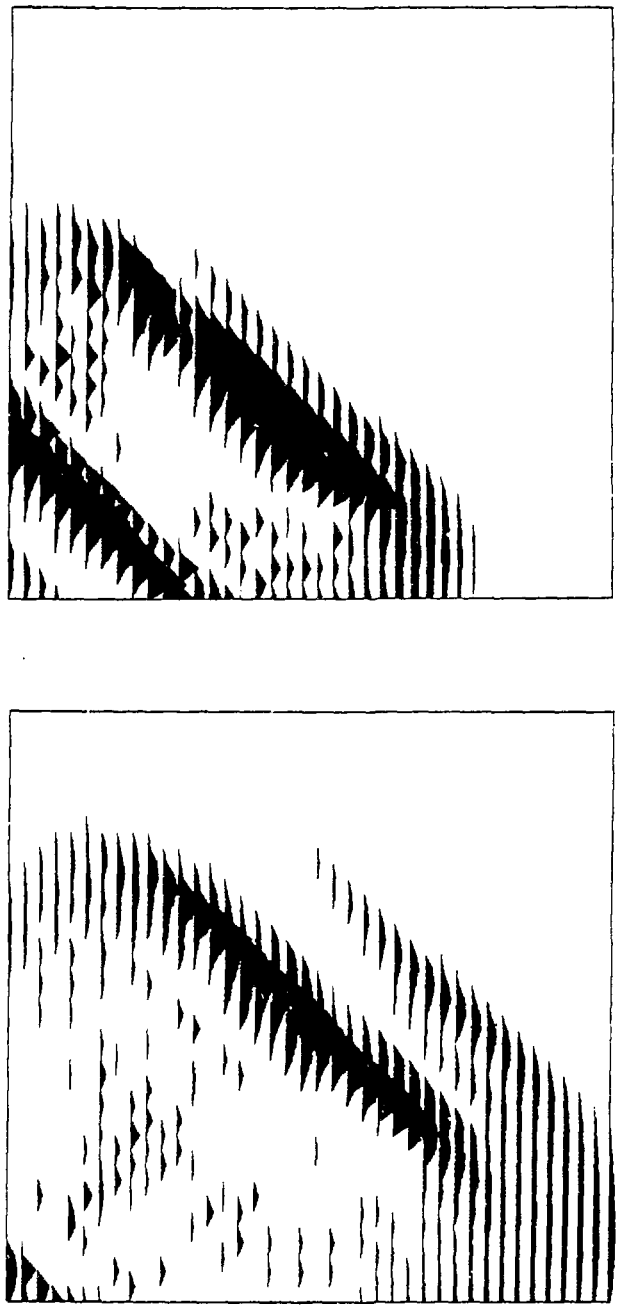

Fig. 5.4.2 (b) PROPAGATING S WAVE. NOTE LEADING P WAVE SLOWLY INCREASING ITS LEAD.

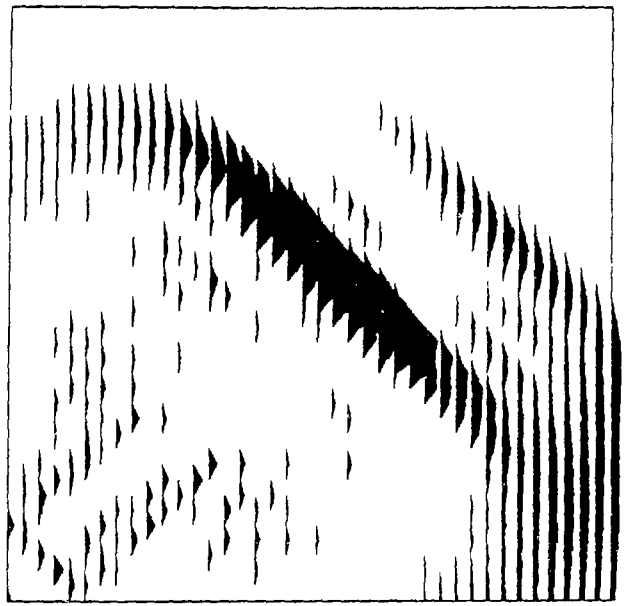

Fig. 5.4.2 (b) CONTINUED

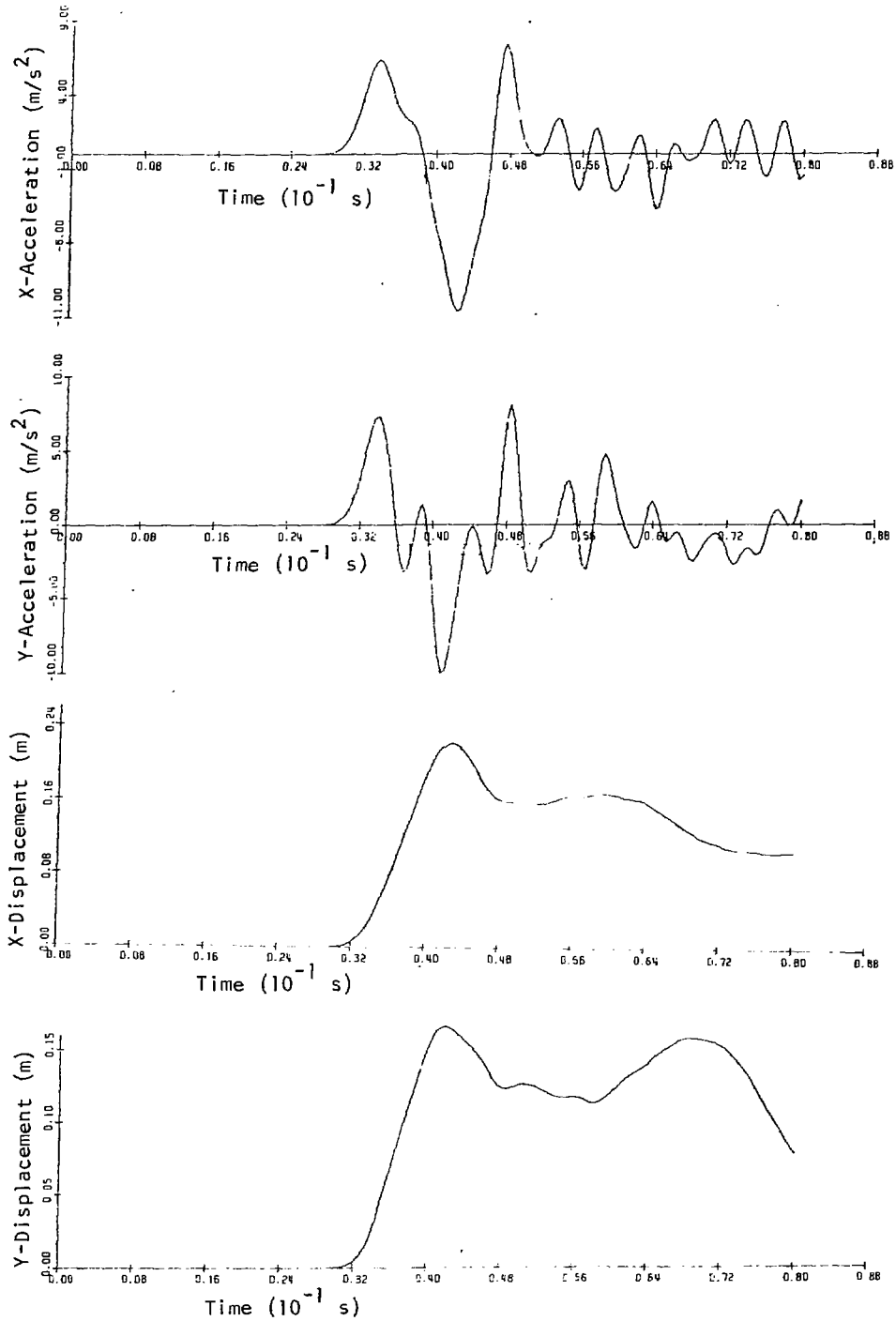

Fig. 5.4.3 TIME HISTORIES OF ACCELERATION AND DISPLACEMENT AT THE SURFACE

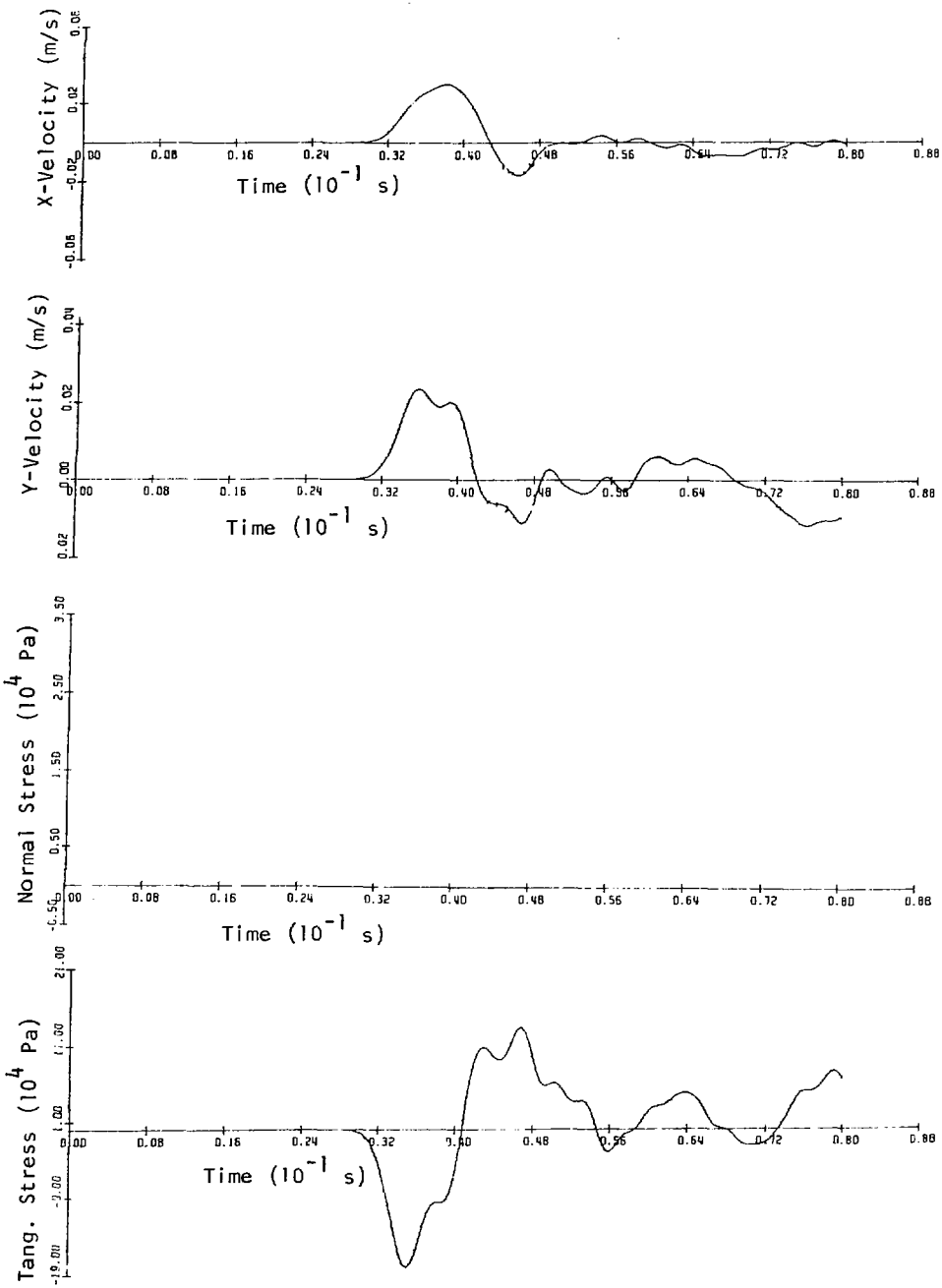

Fig. 5.4.4 TIME HISTORIES OF VELOCITY AND STRESS AT THE SURFACE

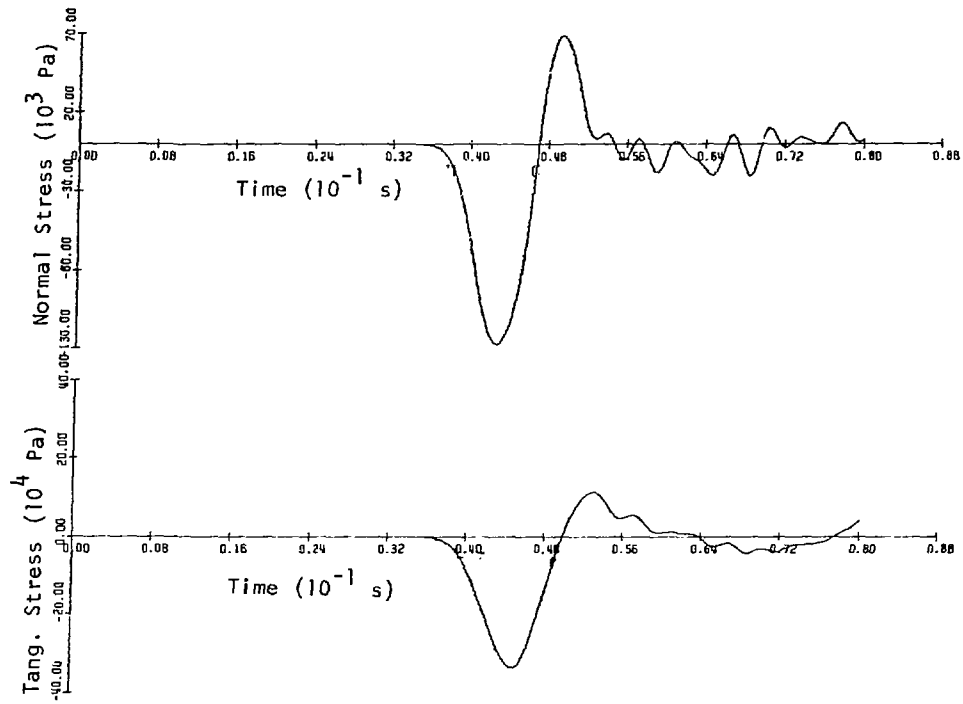

Fig. 5.4.5 STRESS TIME HISTORIES AT ONE GRID POINT IN
FROM THE SURFACE

the convention used in rock mechanics. It should be noted that when the block is in normal and tangential tension it also has a forward velocity. If there were no other factors, such as existing stress, rock support, or self-weight, then this would ensure block movement, provided, of course, that there were existing joints.

The normal stress at the surface remains zero, but the normal stress at the next grid point reaches a magnitude of 0.13 MPa. This creates a maximum stress gradient of 0.026 MPa/m.

The seismic wave has an effective wavelength of about 85 m, which is larger than the supposed tunnel height of 60 m, but it still produces some interesting effects. Lower frequency waves will have a longer wavelength, but will have higher particle velocities and higher stress levels. Shear waves will have shorter wavelengths for a given frequency and higher amplitudes, so it can be seen that they may have a similar effect.

The plots showing displacement do not return to zero after the wave passes. This is solely a result of the way the wave is generated, but it does have some basis in reality. Studies have shown that there are permanent deformations in the vicinity of an earthquake. This has no bearing on the problem being examined, however.

The results presented here can be analyzed in reference to a rock block lodged in a sidewall of the cavern. The stresses generated by the seismic wave are very small, with the maximum tangential tensile stress being 0.16 MPa (24 psi). The accelerations, however, are quite large, being in excess of 1.0 g. When the wave hits the cavern wall, the horizontal and vertical accelerations are in the positive direction, meaning that the block is being driven into the wall and down. The tangential stress is also slightly compressive. However, at around $t = 0.04$ s, the acceleration becomes negative in both directions, meaning that the block is being lifted up and pushed out. At this time, the block still has a forward velocity of about 0.02 m/s.

Provided that the block is unconfined, it will move forward by an unknown amount. If these loading cycles are repeated many times during the course of a single event, then the block will move a significant amount. Again, it should be stated that the consequences of such movement will be highly dependent on the properties of the rock, the stress field and the geometries of joints and cavern.

5.5 CAVERN MODEL

The method of finite differences can now be extended to simulate the conditions surrounding a hypothetical cavern. The shape of the cavern is restricted to rectangular because of the orthogonal nature of the finite-difference grid. Bearing in mind that the purpose of these studies is to establish a methodology for seismic analysis, a rectangle is sufficient until the design has been finalized.

The grid is laid out as a large rectangle, or square, with a smaller rectangle within (Figure 5.5.1). The outer boundaries are both transmitting and absorbing, i.e., they can transmit the free-field seismic

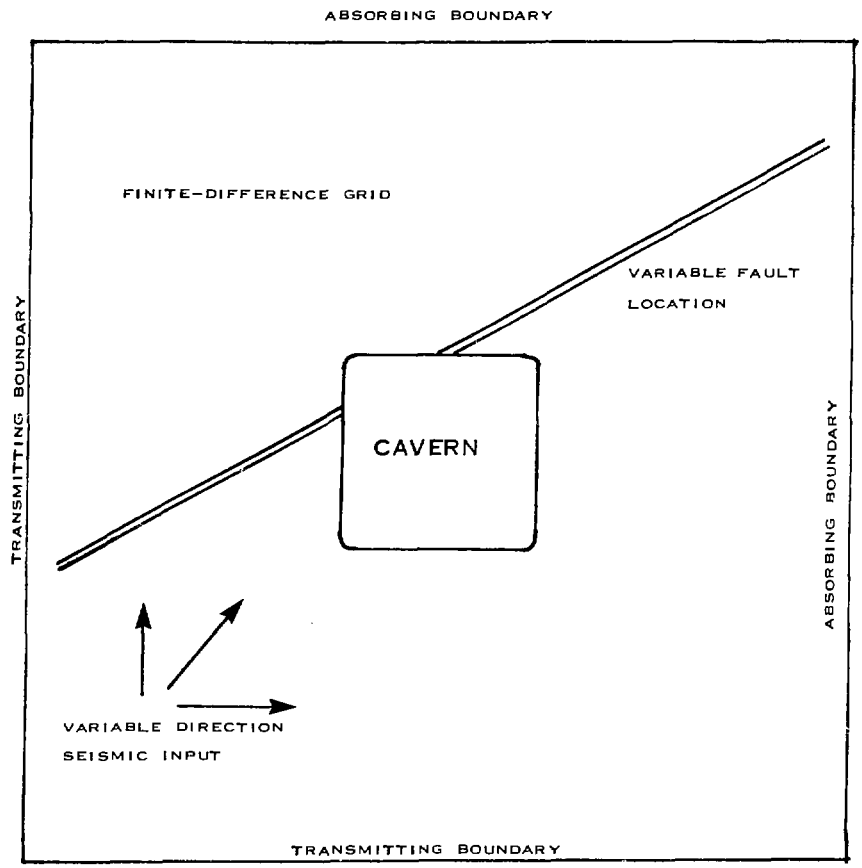

Fig. 5.5.1 COMPUTER MODEL OF DISPOSAL VAULT

input, and can also absorb the return reflections from the cavern. In this manner, they simulate the response of an infinite, two-dimensional medium. The boundary conditions for transmission are calculated by solving the velocity field for seismic plane waves of the two types travelling in any direction. These velocities are then applied at the boundaries. Tests show that both S and P waves can be propagated across the grid in any direction. For most cases, only the left and lower boundaries are used for transmitting.

The boundary conditions of the interior rectangle, or cavern, are those of a free surface. The normal stresses are set to zero and the tangential stresses are adjusted to accommodate this action. With the staggered grid concept, applying realistic boundary conditions remains as one of the more difficult problems to be solved, especially if the chief concern is stability near these boundaries.

One joint or fault at any angle of dip can be located in any position in the model. Thus, it is possible to simulate a joint through the cavern floor where items such as waste canisters might be located, or through the roof to check stability there. The present computer runs have concentrated only on the process of joint rupture itself and not on the problem of triggering by seismic waves.

5.6 INITIAL STRESS CONDITIONS

Of prime importance in setting up the initial conditions is the in situ stress. Based on some published data (Herget, 1974), the stresses at the 1000-m level were chosen to be 50 MPa for the horizontal stress and 25 MPa for the vertical stress. The exact stress values for any vault would, of course, be site-dependent. Shear stresses along discontinuities would tend to decrease if the vertical and horizontal stresses approached equality.

The initial conditions were set by "excavating" the cavern in the stressed grid, with the damping values set very high. The "excavation" consisted of imposing the cavern boundary conditions at $t = 0$. A sufficient number of iterations were run to allow the particle velocities and accelerations to settle to a very low value. The resulting stress contours are plotted in Figures 5.6.1 and 5.6.2. The displacement plot is shown in Figure 5.6.3. Note that the displacements shown by the arrows are magnified 200 times relative to the scale of the cavern. Although this was not the most efficient way to calculate the static solution, it was the only way to obtain all the displacements and stresses at the offset node points so that further dynamic analyses could be carried out.

5.7 CAVERN EXPOSED TO SEISMIC WAVES

The cavern was exposed to seismic plane waves at various angles to test the effect on stresses near the cavern. The input was a piecewise linear velocity pulse, as shown in Figure 5.7.1, with the velocities being applied at the boundaries, compatible with the motions of a travelling plane wave. Although the frequency of the pulse could be decreased by increasing

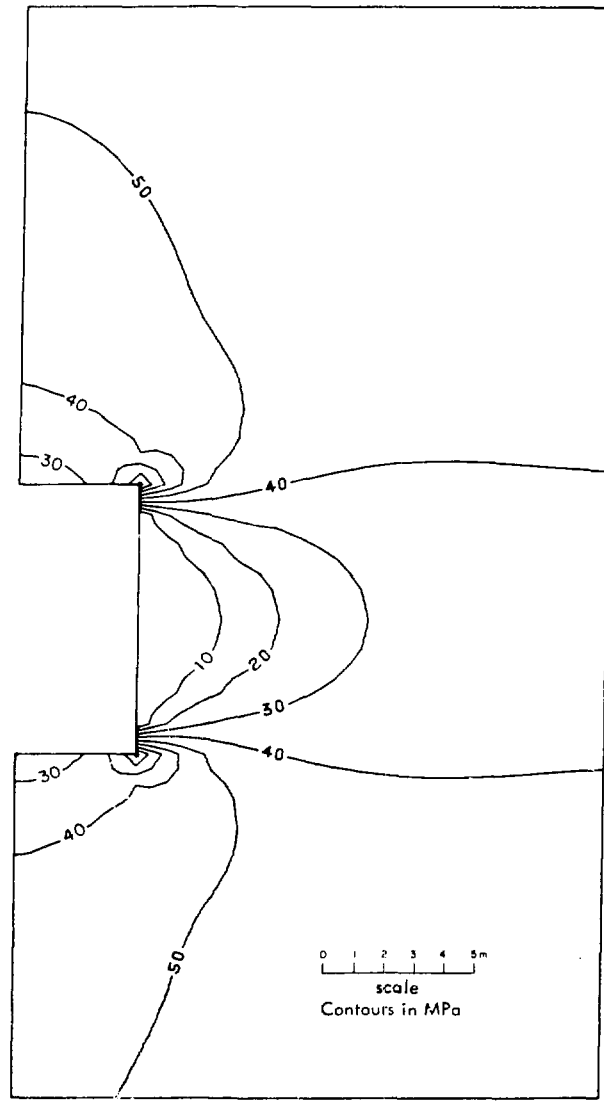

Fig. 5.6.1 HORIZONTAL STRESSES AROUND CAVERN

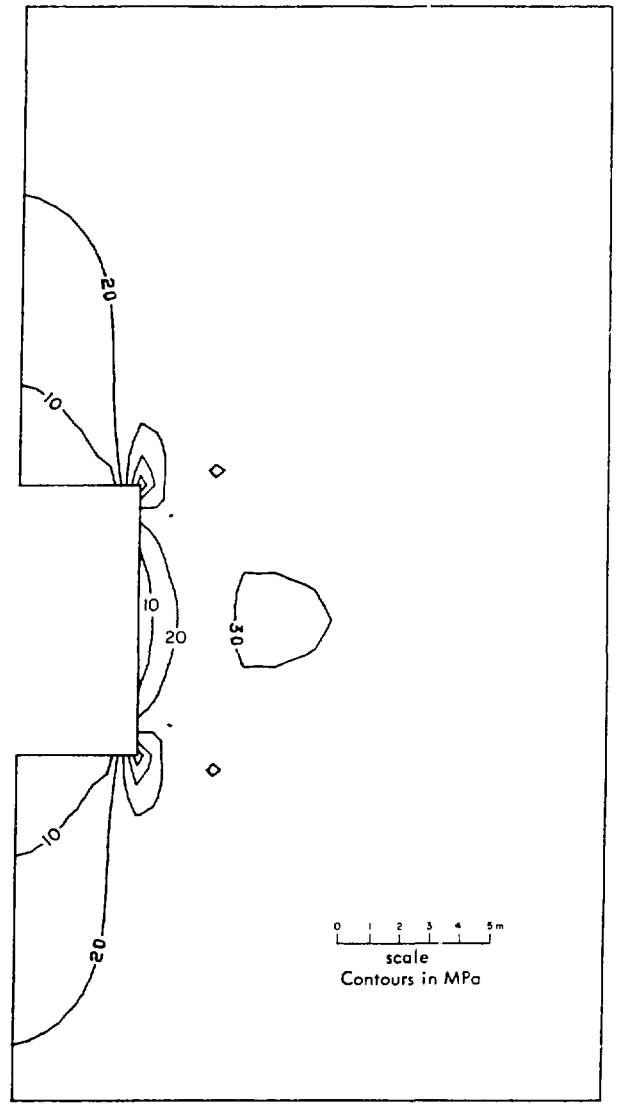

Fig. 5.6.2 VERTICAL STRESSES AROUND CAVERN

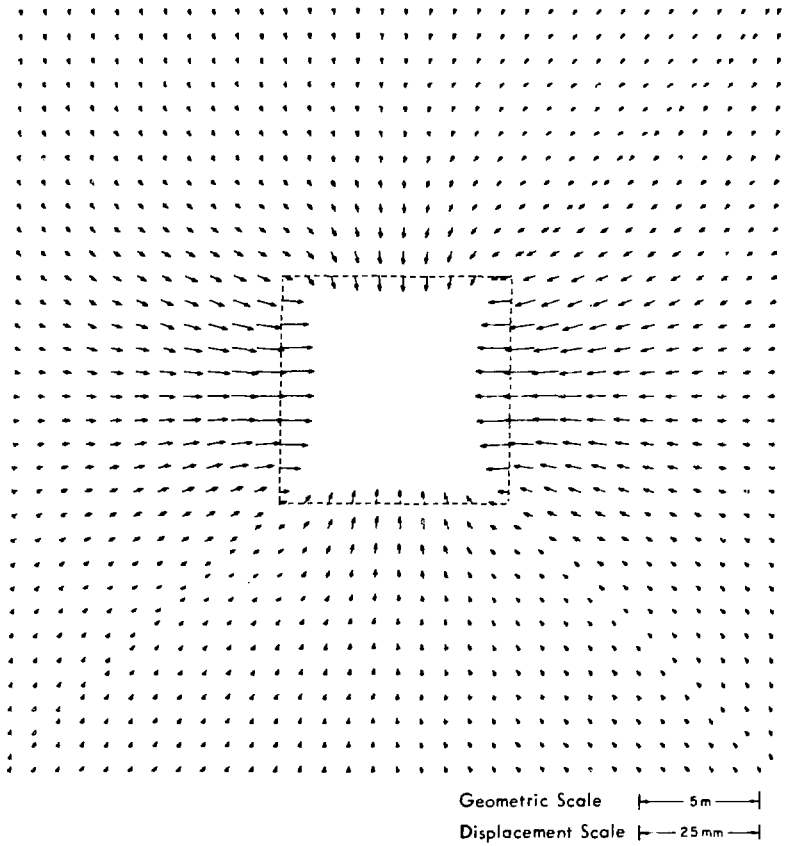

Fig. 5.6.3 INITIAL DISPLACEMENT FIELD AROUND CAVERN

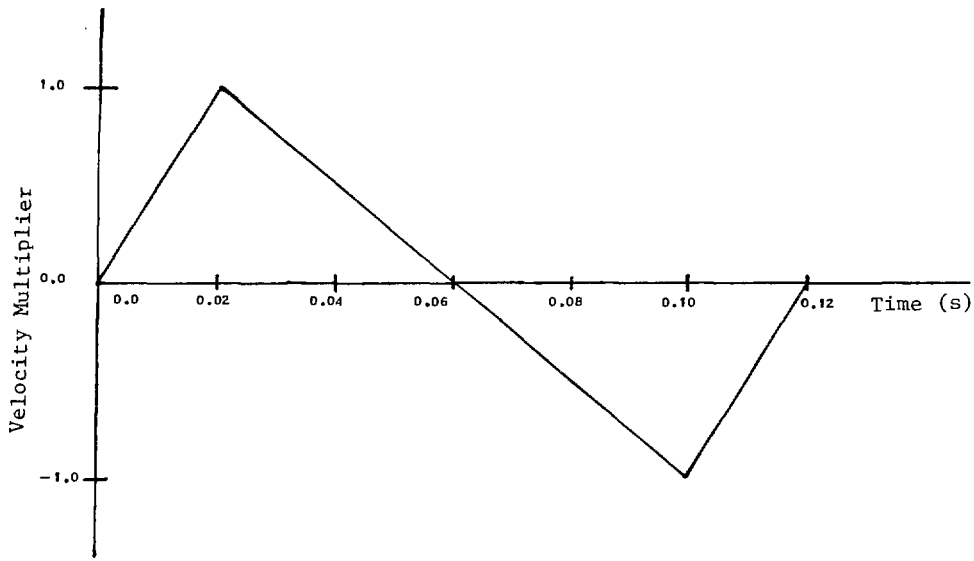

Fig. 5.7.1 NORMALIZED VELOCITY PULSE

the length of time over which it was applied, there is a practical limit determined by the maximum allowable number of iterations. To minimize the cost and to keep the number of iterations down to several hundred, only relatively high-frequency pulses were used.

Figure 5.7.2 shows the accelerations for a horizontal P wave approaching the cavern. The accelerations are about 10 m/s^2 and the stresses away from the cavern are about 1 to 2 MPa. However, as the wave passes the stresses at the cavern wall fluctuate by only a fraction of a MPa. In general, for the seismic waves tested, the stresses at the cavern surfaces were about one tenth of the regional seismic stresses.

Simulations were also run using horizontal P waves, vertical P waves, vertical S waves and horizontal S waves. Although the stresses generated by the input waves are small, it appears that the stresses at the cavern are very small in relation to the in situ stresses.

Another way to look at the effect of seismic waves is to check the effect on the Mohr-Coulomb failure criterion which can be expressed as:

$$S_i = S_o$$

where $$S_i = \sigma_1[(\mu^2 + 1) - \mu] - \sigma_3[(\mu^2 + 1) + \mu]$$

In this formulation, S_o is the characteristic cohesion of the rock, determined by actual testing (not to be confused with C_o, the uniaxial compressive strength, using the notation of Jaeger and Cook, 1976), and μ is the coefficient of friction. Assuming a value for μ, S_i is the cohesion that the rock mass must have to prevent failure. If S_i is greater than or equal to S_o, failure will occur. If the S_o value is that for a joint instead of the intact rock mass, then failure would only occur for an optimally oriented rock joint. A plot of S_i around an underground opening is shown in Figure 5.7.3.

When the cavern is exposed to seismic waves, the values of S_i change. Values of S_i are shown for instants in time for a horizontal P wave in Figure 5.7.4. It can be seen that the maximum increase for S_i is 0.2 MPa. This is most likely not significant when compared with other influences affecting a rock excavation, such as nearby blasting and machinery vibration.

5.8 JOINT RUPTURE

Once the joint was defined in the computer model by giving an intercept and a dip, it was allowed to rupture under the in situ stresses. Rupture was sometimes not easy to accomplish. If the initial angle of friction were set too high, then there would be no activity at all. Even if the value of μ was low enough to initiate rupture, sometimes only the first one- or two-grid points would shift, corresponding to a small burst. Only if the critical displacement were set small enough and the minimum friction angle were set low enough would large scale rupture take place.

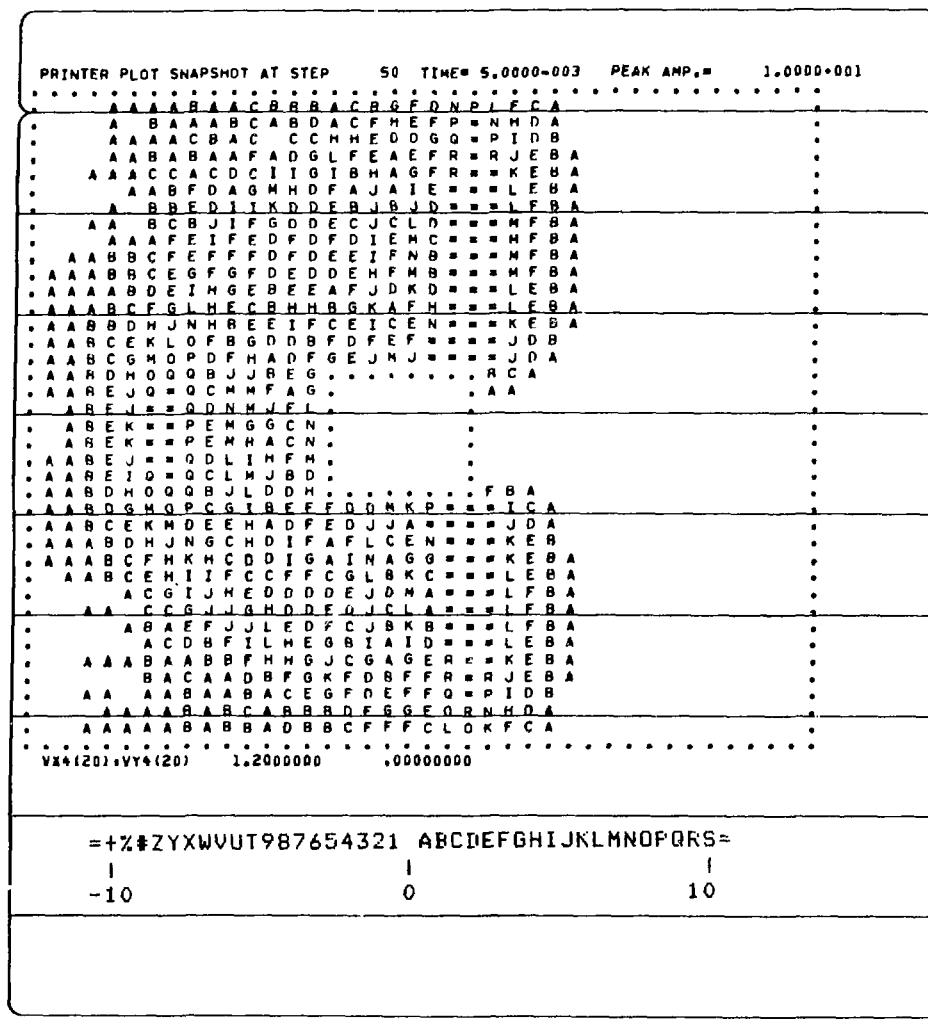

Fig. 5.7.2 ACCELERATIONS FOR A HORIZONTAL P WAVE

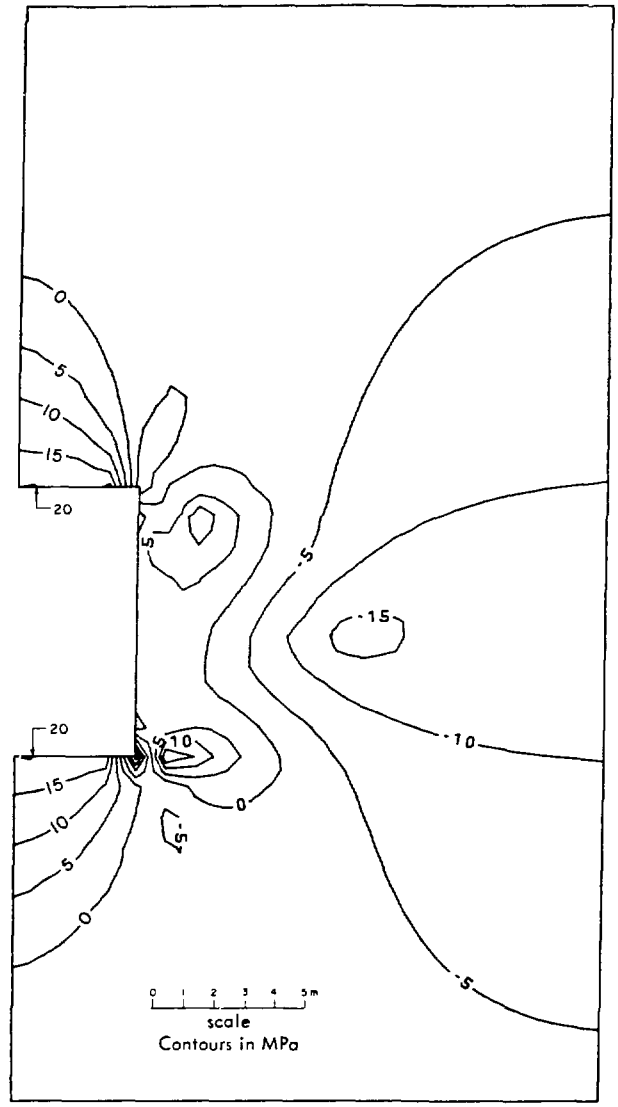

Fig. 5.7.3 REQUIRED COHESION VALUES, S_i

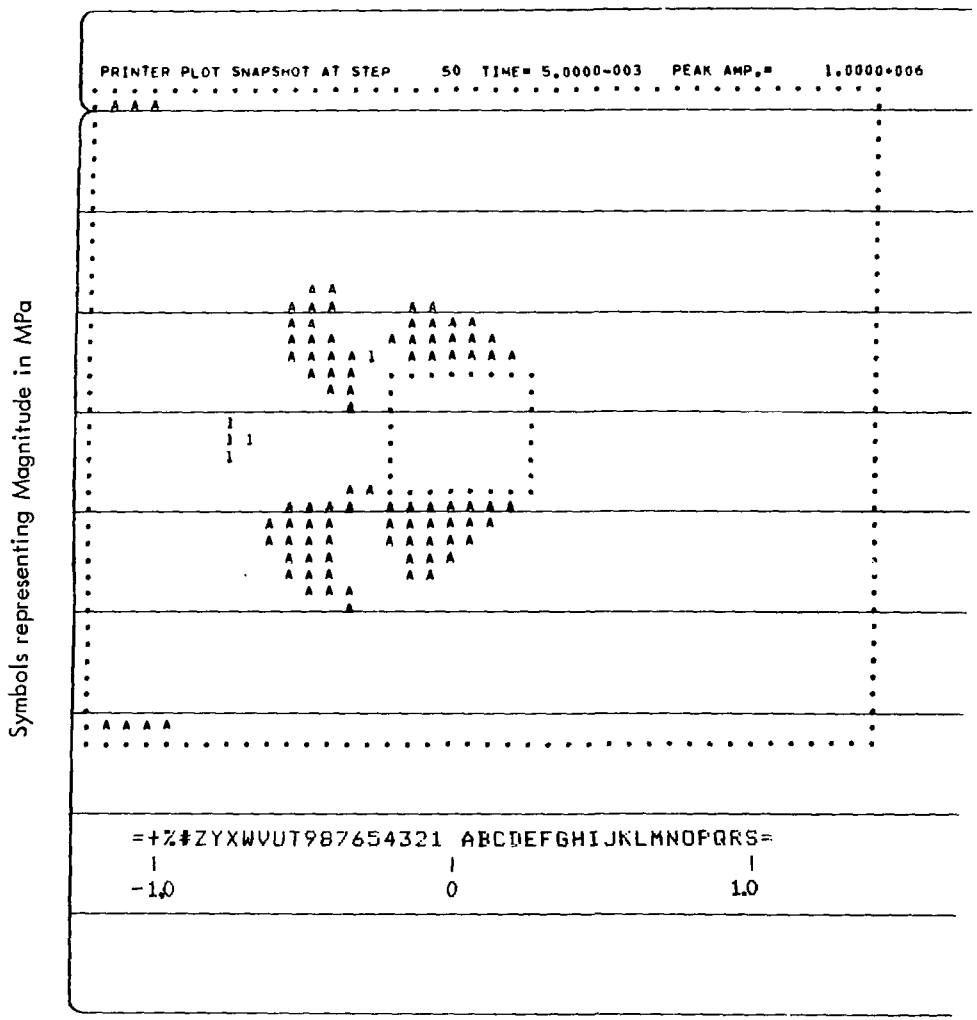

Fig. 5.7.4 (a) CHANGE IN S_1 FOR HORIZONTAL P WAVE AT $t = 0.005\,s$

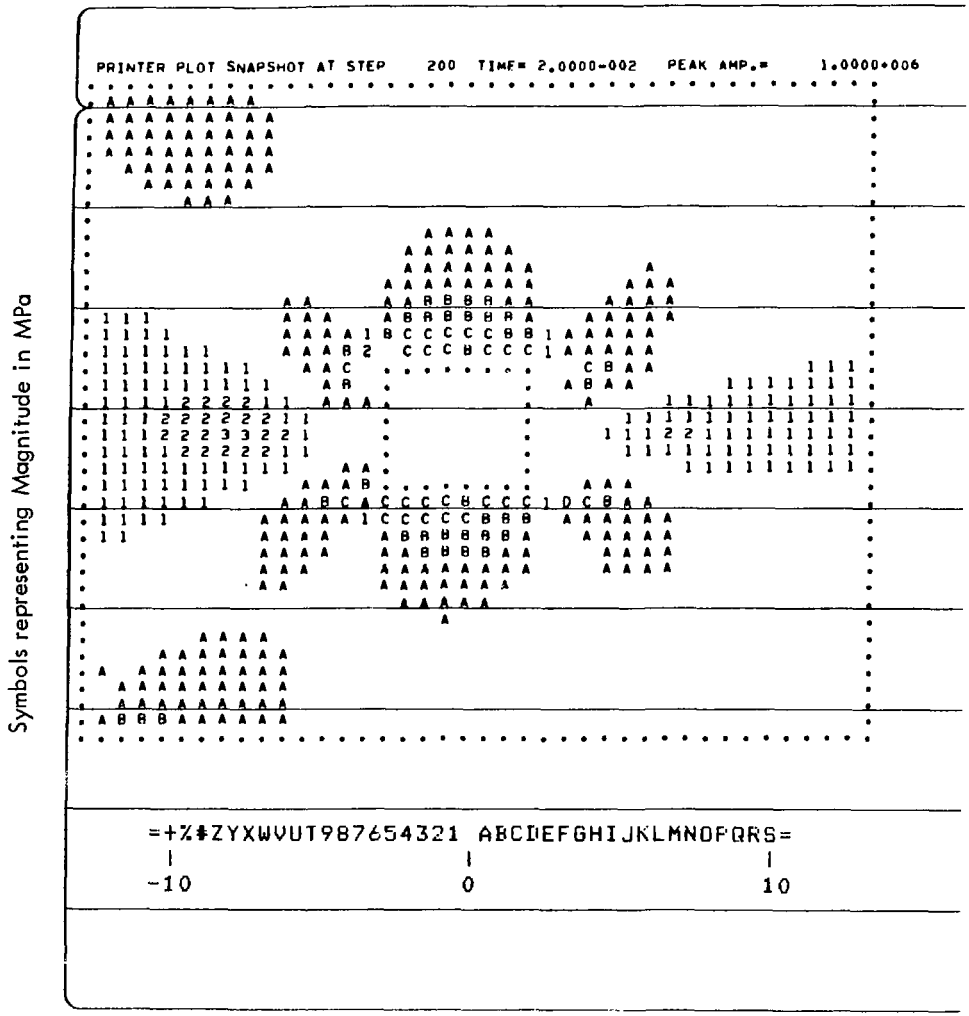

Fig. 5.7.4 (b) CHANGE IN S_i FOR HORIZONTAL P WAVE AT t=0.02s

Figures 5.8.1 and 5.8.2 show displacement fields while rupture is taking place. The first (Figure 5.8.1) shows the magnified displacements before any joint movement, and is due to the in situ stress alone. The other plot (Figure 5.8.2) shows the displacements for a joint at a low angle and for a friction angle that drops to 0.6 of the static value. These "snapshots" were taken after 50 iterations after the start of the rupture, or at t = 0.005 s.

Note that these pictures show evidence of "curled" displacements or swirls, which are seismic waves propagating away from the disruption.

It was found that, in general, for significant rupture to occur, the critical displacement had to be quite small, about 0.1 mm, and the minimum coefficient of friction had to be zero. It is not known what these values are in the field, but a high value of the critical displacement and a small amount of dynamic friction reduction would ensure stability with respect to disruptive events.

6. SUMMARY AND RECOMMENDATIONS

The following observations and deductions are based on the studies reported here:

(a) Case histories demonstrate that underground installations are not very susceptible to damage from seismic motions, primarily because they are very stiff structures and do not undergo resonance, which is the chief agent of destruction for surface structures. Damage only occurs if a fault intersects a tunnel, which is an example of near-field motion. Damage would most likely occur if a fault ruptured very close to a facility, although tunnels in South Africa have not been damaged by near-field, high-acceleration (12 g) seismic events.

(b) Little is known about the stresses associated with seismic waves; however, evidence points to the fact that stresses are a limiting factor with seismic waves. Near a fault rupture, accelerations may be very high, but only at high frequencies. This implies a limit to stress, since stress decreases for high frequencies. High accelerations at high frequencies but low stress are not expected to damage a well-constructed underground opening.

(c) Seismic waves from distant sources are not expected to generate large stresses around underground openings, since high stress waves would be rapidly attenuated. The induced seismic stresses would only be a small percentage of the excavation stresses, and would, in all probability, have no effect on the rock, except to act as a trigger for some extremely sensitive failure mechanism. A major unknown is whether such a failure mechanism can exist and survive the other disturbances such as thermal loading and general vibrations.

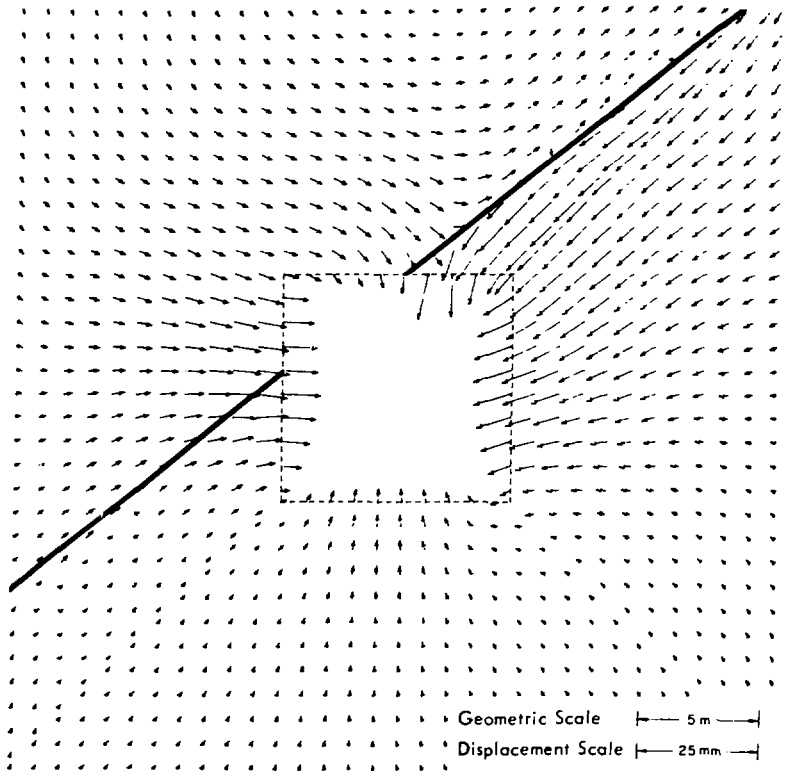

Fig. 5.8.1 FINAL DISPLACEMENT FIELD WITH 40° JOINT

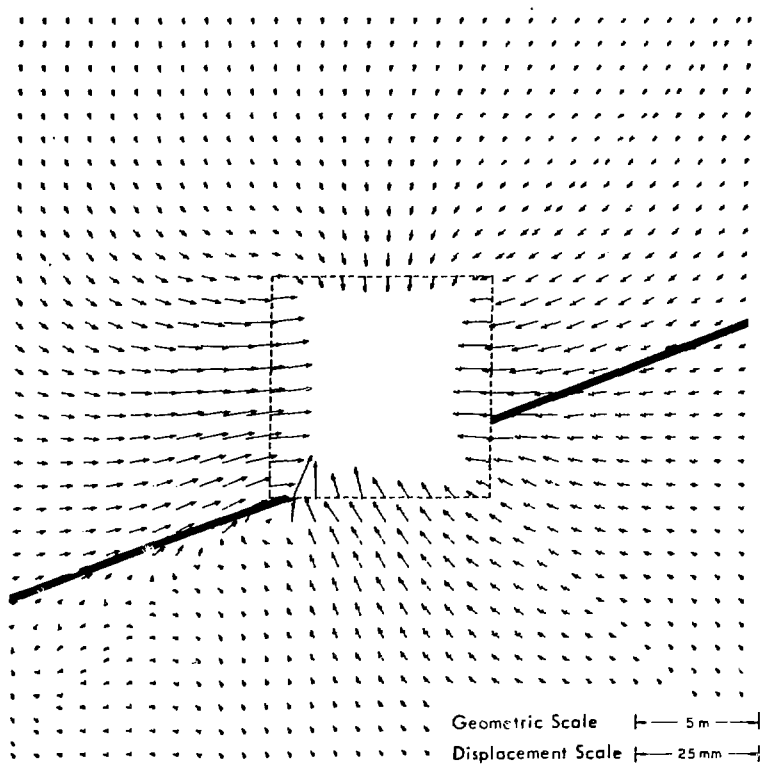

Fig. 5.8.2 FINAL DISPLACEMENT FIELD WITH 20° JOINT

(d) Cavern seismic response is dependent on the effects of wave interaction with both the surface and the cavern complex. The effect of interaction with the ground surface is to reduce the peak acceleration with depth. Provided that the peak accelerations of the incoming seismic waves occur in pulses, there will be a decrease of the surface amplification with depth, i.e. an effective attenuation of peak accelerations with depth. The amount and rate of decrease depend on many factors, the most important being the frequency and the angle of incidence of the incoming seismic waves. This decrease is complete at a depth of about one fourth of the effective wavelength of the disturbance. This depth is typically around 100 to 300 m for most frequencies of interest. Taking other factors, such as the effect of non-vertical incidence, into account, the surface amplification factor in rock can be as high as 2.0, but a more reasonable average might be 1.5. If an earthquake source is directly below and closer than about 1 km, then the seismic motions may increase with depth.

(e) Since the underground opening is in a stressed regime, dynamic rupturing along an existing stressed joint or other discontinuity may be possible. Such an event could be triggered by seismic motions or could occur spontaneously. Computer simulation shows that seismic waves add only a small amount of stress to existing stresses and are unlikely to be a triggering mechanism. Allowing the discontinuities to rupture has demonstrated that the adhesion parameters of critical displacement and minimum angle of friction have a significant influence on stability.

(f) Rock support, be it rock bolts or lining, is not expected to change the seismic stresses that a cavern might experience. Also, once a disruptive event commences, no support could be expected to hold in the immediate area. Support would only be expected to increase the safety factor of the discontinuities, i.e., make them less susceptible to rupture. However, due to the extremely stiff nature of the rock compared to the flexibility of a support system, it would be difficult to find an adequate support method.

The best defense against dynamic disruptions appears to be proper design, including a cavern shape and direction that would minimize the stress on discontinuities. For excavation, tunnel boring machines may be better than blasting, to ensure minimum disturbance of the discontinuities.

ACKNOWLEDGEMENTS

The author wishes to acknowledge his Ontario Hydro and AECL colleagues, in particular Dr. C.F. Lee and Mr. E.M. Taylor, for their helpful discussions and review. Many thanks also to those who helped prepare this report, especially the Geotechnical Drafting Section and Ontario Hydro Word Processing Centre Services.

REFERENCES

Aki, K. 1968. Seismic consideration in siting large underground openings in rock. Ph.D. thesis, University of California, Berkeley.

Allensworth, J.A., J.T. Finger, J.A. Milloy, W.B. Murfin, R. Rodeman, and S.G. Vandevender. 1977. Underground siting of nuclear power plants: potential benefits and penalties. Sandia Laboratories Report, SAND-76-0412.

Anderson, D.L., and R.S. Hart. 1978. Q of the earth. J. Geophys. Res. 83, no. B12, 5869-5882.

Asmis, G.J.K. 1981. Personal communication.

Barton, N., and H. Hansteen. 1979. Large underground openings at shallow depth: comparison of deformation magnitudes from jointed models and linear elastic F.E. analyses. *Norwegian Geotechnical Institute Internal Report No. 54205-5.*

Basham, P.W. 1975. Design basis ground motion for Darlington Nuclear Generating Station A. Seismological Services of Canada Internal Report No. 75-16.

Berkey, C.P. 1945. A geological study of the Massena - Cornwall earthquake of September 5, 1944 and its bearing on the proposed St. Lawrence River project. United States Engineer Office, New York District.

Boatwright, J. 1978. Detailed spectral analysis of two small New York State earthquakes. Seismol. Soc. Amer. Bull. 68, 1117-1131.

Bolt, B.A., and R.A. Hansen. 1977. The upthrow of objects in earthquakes. Seismol. Soc. Amer. Bull. 67, 1415-1427.

Bolt, B.A. 1978. Earthquakes: a primer. W.H. Freeman and Company, Reading, England.

Bowden, F.P., and D. Tabor. 1964. The friction and lubrication of solids. Vol. 2, Clarendon, Oxford.

Dieterich, J.H. 1972. Time-dependent friction in rocks. J. Geophys. Res. 77, 3690-3697.

Dieterich, J.H. 1978. Time-dependent friction and the mechanics of stick-slip. Pure Appl. Geophys. 116, 790-806.

Dieterich, J.H. 1979. Modelling of rock friction, 1, experimental results and constitutive equations. J. Geophys. Res. 84, 2161-2168.

Dowding, C.H., and A. Rozan. 1978. Damage to rock tunnels from earthquake shaking. J. Geotech. Eng. Div., ASCE 104, 175-191.

Duke, C.M., and D.J. Leeds. 1959. Effects of earthquakes on tunnels. In Protective construction in a nuclear age. Vol. 1, Proceedings of the second protective construction symposium, Santa Monica, California, J.J. O'Sullivan, editor. MacMillan Co., New York, pp. 303-328.

Hartzell, S.H., J.N. Brune, and J. Prince. 1978. The October 6, 1974 Acapulco earthquake: an example of the importance of short-period surface waves in strong motion. Seismol. Soc. Amer. Bull. 68, 1663-1667.

Herget, G. 1974. Ground stress determinations in Canada. Rock Mech., Austria 6, 53-64.

Iwasaki, T., S. Wakabayashi, and F. Tatsuoka. 1977. Characteristics of underground seismic motions at four sites around Tokyo Bay. U.S. Nat. Bur. Stand., Spec. Publ. No. 477, pp. 111.41-111.56.

Jaeger, J.C., and N.G.W. Cook. 1976. Fundamentals of rock mechanics. Chapman and Hall, London.

Kachadoorian, R. 1965. Effects of the earthquake of March 27, 1964, at Whittier, Alaska. United States Geological Survey Professional Paper, 542-B, p. B1-B21.

Kanasewich, E.R. 1975. Time sequence analysis in geophysics. University of Alberta Press.

Lysmer, J., and R.L. Kuhlemeyer. 1969. Finite dynamic model for infinite media. ASCE - Proc. 95 (J. Eng. Mechanics Div.) EM4, 859-877.

McGarr, A., R.W.E. Green, and S.M. Spottiswoode. 1980. Strong ground motions of mine tremors: some implications for near-source ground motion parameters. South African Chamber of Mines Report No. 32/80.

Milne, W.G., and A.G. Davenport. 1969. Distribution of earthquake risk in Canada. Seismol. Soc. Amer. Bull. 59, 729-754.

Prater, A.B., and C.D. Wieland. 1976. Response of structures embedded in the ground to travelling seismic waves. International Symposium on Earthquake Structural Engineering, St. Louis, Missouri.

Scholz, C.H., P. Molnar, and T. Johnson. 1972. Detailed studies of the frictional sliding of granite and implications for the earthquake mechanism. J. Geophys. Res. 77, 6392-6406.

Sibson, R.H. 1977. Kinetic shear resistance, fluid pressures and radiation efficiency during seismic faulting. Pure Appl. Geophys. (Switzerland) 115, 387-400.

Smith, R.B., P.L. Winkler, J.G. Anderson, and C.H. Scholz. 1974. Source mechanism of microearthquakes associated with underground mines in eastern Utah. Seismol. Soc. Amer. Bull. 64, 1295-1317.

Stevens, P.R. 1977. A review of the effects of earthquakes on underground mines. United States Geological Survey Open-file Report No. 77-313.

Teufel, L.W., and J.M. Logan. 1978. Effect of displacement rate on the real area of contact and temperatures generated during frictional sliding of Tennessee sandstone. Pure Appl. Geophys. (Switzerland) 116, 840-865.

APPENDIX

CONVOLUTION BY z TRANSFORMATION

This method considers convolution as the coefficients obtained from a multiplication of two polynomials. For wavelets $\bar{w}$ and $\bar{x}$, which are represented by two series of points defining the digitized waves:

$$\bar{w} = (w_0, w_1, w_2, \ldots) \qquad \bar{x} = (x_0, x_1, x_2, \ldots),$$

two polynomials W and X are formed as follows:

$$W(z) = w_0 + w_1 z + w_2 z^2 + \ldots$$

$$X(z) = x_0 + x_1 z + x_2 z^2 + \ldots$$

where z is a complex number.

A single algorithm for multiplying two polynomials can be implemented on a computer. It is then only necessary to input the two waveforms to be convoluted, assume that the digitized amplitudes are coefficients of polynomials, and multiply them together. The final product is the coefficients of the resulting polynomials, keeping in mind the power of z to which the coefficient belongs.

ISSN 0067-0367

To identify individual documents in the series we have assigned an AECL- number to each.

Please refer to the AECL- number when requesting additional copies of this document from

Scientific Document Distribution Office
Atomic Energy of Canada Limited
Chalk River, Ontario, Canada
KOJ 1JO

Price: $5.00 per copy

ISSN 0067-0367

Pour identifier les rapports individuels faisant partie de cette série nous avons assigné un numéro AECL- à chacun.

Veuillez faire mention du numéro AECL -si vous demandez d'autres exemplaires de ce rapport au

Service de Distribution des Documents Officiels
L'Energie Atomique du Canada Limitée
Chalk River, Ontario, Canada
KOJ 1JO

prix: $5.00 par exemplaire